PAPER

Electromagnetic forced vibrations of composite nanoplates using nonlocal strain gradient theory

To cite this article: Mohammad Malikan *et al* 2018 *Mater*. *Res. Express* **5** 075031

View the article online for updates and enhancements.

Materials Research Express

CrossMark

Electromagnetic forced vibrations of composite nanoplates using nonlocal strain gradient theory

Mohammad Malikan[1,4] , **Van Bac Nguyen**[2] and **Francesco Tornabene**[3]

1   Department of Mechanical Engineering, Faculty of Engineering, Islamic Azad University, Mashhad Branch, Mashhad, Iran
2   Department of Mechanical Engineering and the Built Environment, College of Engineering and Technology, University of Derby, Derbyshire, United Kingdom
3   Department of Civil, Chemical, Environmental, and Materials Engineering, University of Bologna, Bologna, Italy
4   Author to whom any correspondence should be addressed.

E-mail: mohammad.malikan@yahoo.com, vb.nguyen@derby.ac.uk and francesco.tornabene@unibo.it

Abstract

This article is intended to analyze forced vibrations of a piezoelectric-piezomagnetic ceramic nanoplate by a new refined shear deformation plate theory in conjunction with higher-order nonlocal strain gradient theory. As both stress nonlocality and strain gradient size-dependent effects are taken into account using the higher-order nonlocal strain gradient theory, the governing equations of the composite nanoplate are formulated. When the nanoplate is subjected to a transverse harmonic loading and all the edges are considered as simple boundaries, the governing equations can be solved with a closed-form solution, from which the maximum dynamic deflections are obtained. To validate the results of the new proposed plate theory, the comparisons between ours and the well-known papers in the literature are presented. The influences of different nonlocal parameters and material properties on the nanoplate's dynamic responses are also studied.

1. Introduction

Due to their amazing features such as high temperature stability, high strength and high corrosion resistance, special magnetic and electrical properties (piezoelectricity, superconductivity, insulating or semiconducting and etc), the advanced nanoceramics are on the list of the crucial and strategic components in many industries. For example, in the aerospace industry, the resistance of these materials against heat is so important, and also in the electronic and communications industries, due to their good optical and electrical properties, they are considered as important components [1, 2].

$BaTiO_3$ is one of the useful nanoceramics for various applications. The experimental studies on this material showed that it has excellent optical properties [3, 4] and also structural studies showed its amazing elastic and heat properties [5]. It is interesting when we got the electromagnetic nanostructure by combining $BaTiO_3$ with $CoFe_2O_4$ in order to achieve novel materials. During the past decade such a material was made by routine industrial ceramic manufacturing methods within which the new material has both magnetic and electric reactions in its molecular structures [6–10]. Of course, considering mechanical behavior of such a new material can have advantages for advanced industries. Although there have been a wide range of studies about assessing mechanical behavior of nanostructures, electromagnetic nanostructures have been far from the attention of researchers around the world yet. This might be because of complicate behavior of such materials that leads to complex computational formulation to examine them. Ke *et al* [11] modeled a piezoelectric nanobeam on the basis of nonlocal elasticity theory of Eringen. They studied natural frequencies for thick nanobeams. In another study, Ke *et al* [12] investigated stability and post stability of piezoelectric nanobeams in electrical and thermal environments. Critical buckling loads and natural frequencies of nanoplates included piezoelectricity were evaluated by Jiang and Yan [13]. In a special case, Fang and Zhu [14] embedded a nonhomogeneous shell in a medium with piezoelectricity property and calculated its natural frequencies. Fang *et al* [15] studied the impact

of surface energy for orthotropic tube nanoshells and its nonlinear frequencies were computed. Bidirectional stability of natural frequencies of double-layered nanoplates rested on visco-Pasternak substrate were analyzed in electrical and magnetic environments by Jamalpoor *et al* [16]. Their problem was modelled by classical plate theory and nonlocal elasticity one. Post stability of a rectangular nanoplate incorporates both electrical and magnetic properties was investigated by Gholami and Ansari [17]. They applied higher-order shear deformations theories by using various functions such as Parabolic, Trigonometric, Hyperbolic and Exponential for several boundary conditions. The nonlocal elasticity theory of Eringen was accompanied with the equations and generalized differential quadrature method was employed to calculate the deflections of post buckling. Arefi and Zenkour [18] dynamically modeled a nanocomposite plate in electrical and magnetic environments which was placed on a visco-Pasternak medium. Natural frequencies were obtained whilst the small scale effects were considered by nonlocal continuum theory. Barati and Shahverdi [19] presented forced vibration of a heterogeneous nanoporous plate by combining a modified shear deformation plate theory and lower-order strain gradient model. Galerkin's method was considered to solve the equations. Ebrahimi and Barati [20] studied damping vibration of graphene sheets by applying lower-order strain gradient theory on a higher-order refined plate theory. The DQM was used to obtain numerical results for fully simply supported boundary conditions. Also, there have been done many valuable research within which the nanostructures have been investigated in various conditions [21–35].

This work provides and reports a new refined first-order shear deformation theory to assess excitation frequencies for electromagnetic nanoplates. The nanoplate is exposed to a transverse dynamic harmonic load and stayed in electrical and magnetic environments. By using nonlocal strain gradient theory the stress nonlocality and strain gradient size-dependent effects are taken into account. Moreover, the Navier solution technique is applied to solve the forced vibration equations considering fully simply-supported edges. Eventually, the dynamic deflections are obtained for various conditions and some new results are presented in this category.

2. Mathematical modeling

2.1. A new one variable shear deformation plate theory (OVFSDT)

Figure 1 illustrates a continuum nanoplate which is subjected to magnetic (ψ_0) and electric (φ_0) fields on its upper and lower layers. A transverse dynamic load uniformly acted on the nanoplate $q(t)$. The three-dimensional picture of the nanoplate shows L_x for its length, L_y for its width, and h represents its thickness, respectively.

Initially, according to the first-order shear deformation theory (FSDT), the displacement field of the nanoplate can be defined as follows [36]:

$$\begin{Bmatrix} U(x, y, z, t) \\ V(x, y, z, t) \\ W(x, y, z, t) \end{Bmatrix} = \begin{Bmatrix} u(x, y, t) + z\varphi(x, y, t) \\ v(x, y, t) + z\psi(x, y, t) \\ w(x, y, t) \end{Bmatrix} \tag{1}$$

In which u, v and w are the displacement vectors of mid-surface in x, y and z directions, respectively. In addition, for the angles of rotation of the elements of the nanoplate around y and x axis, φ and ψ are defined, respectively. First, let us reconsider the simple first-order shear deformation theory (S-FSDT) within which it was assumed [37–42]:

$$w = w(bending) + w(shear) \tag{2}$$

Moreover, the φ and ψ angles were expressed as follows:

$$\begin{Bmatrix} \varphi \\ \psi \end{Bmatrix} = \begin{Bmatrix} -\dfrac{\partial w_b}{\partial x} \\ -\dfrac{\partial w_b}{\partial y} \end{Bmatrix} \tag{3}$$

Substituting equations (2), (3) in equation (1) the displacement field of the S-FSDT is presented [37–42]:

$$\begin{Bmatrix} U(x, y, z, t) \\ V(x, y, z, t) \\ W(x, y, z, t) \end{Bmatrix} = \begin{Bmatrix} u(x, y, t) - z\dfrac{\partial w_b(x, y, t)}{\partial x} \\ v(x, y, t) - z\dfrac{\partial w_b(x, y, t)}{\partial y} \\ w_b(x, y, t) + w_s(x, y, t) \end{Bmatrix} \tag{4}$$

Figure 1. (a) Composite nanoceramics plate subjected to magnetic and electric fields in 3D Cartesian coordinate system, (b) Distribution of the transverse dynamic load on the nanoplate.
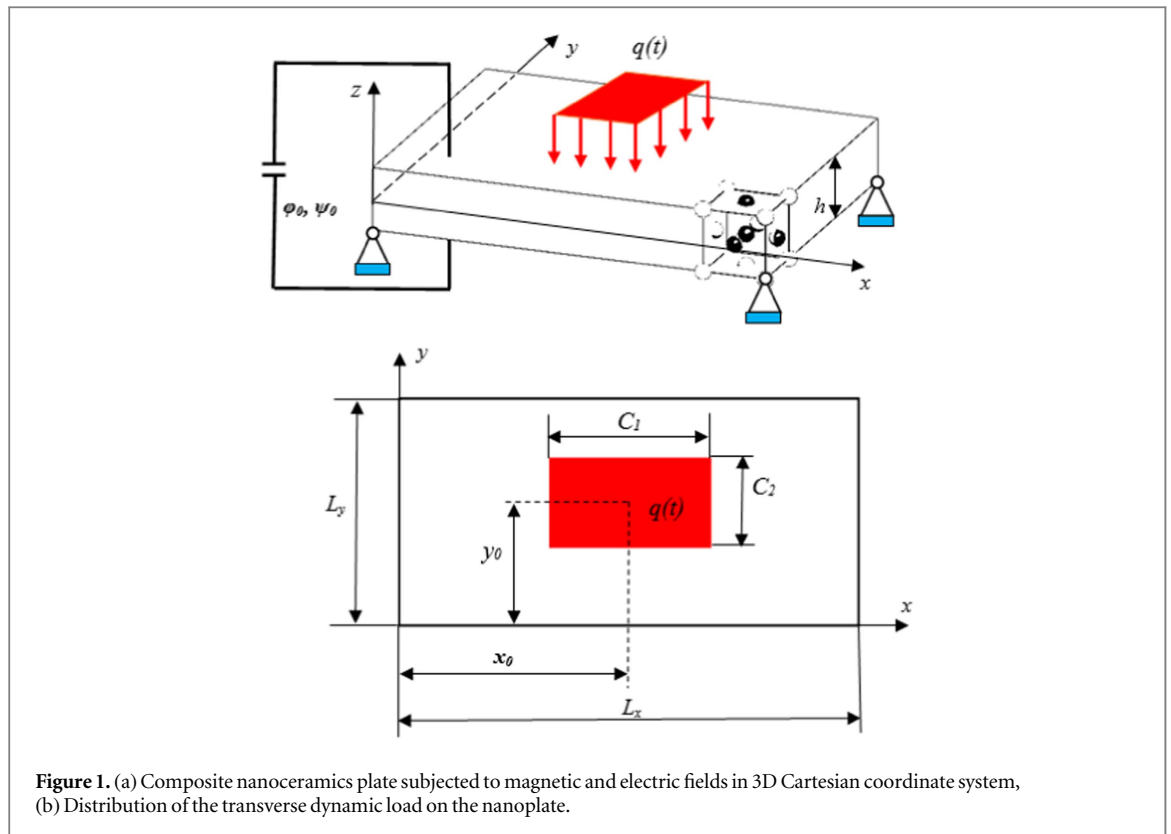
The expression $w = w_b + w_s$ might lead to some ambiguities, since the visualization of shear deflection is hard. That's why, equation (5) would be refined:

$$\begin{Bmatrix} U(x, y, z, t) \\ V(x, y, z, t) \\ W(x, y, z, t) \end{Bmatrix} = \begin{Bmatrix} u(x, y, t) - z\dfrac{\partial w_b(x, y, t)}{\partial x} \\ v(x, y, t) - z\dfrac{\partial w_b(x, y, t)}{\partial y} \\ w_b(x, y, t) + W' \end{Bmatrix} \tag{5}$$

As it is clear, the bending deflection is a conceptual item to capture the parametric value of the shear deflection. So, the bending deflection can be used to find the non-numerical value of w_s:

$$\begin{bmatrix} N_{xx} \\ N_{yy} \\ N_{xy} \\ M_{xx} \\ M_{yy} \\ M_{xy} \\ Q_y \\ Q_x \end{bmatrix} = \begin{bmatrix} A_{11} & A_{12} & 0 & 0 & 0 & 0 & 0 & 0 \\ A_{21} & A_{22} & 0 & 0 & 0 & 0 & 0 & 0 \\ 0 & 0 & A_{66} & 0 & 0 & 0 & 0 & 0 \\ 0 & 0 & 0 & D_{11} & D_{12} & 0 & 0 & 0 \\ 0 & 0 & 0 & D_{21} & D_{22} & 0 & 0 & 0 \\ 0 & 0 & 0 & 0 & 0 & D_{66} & 0 & 0 \\ 0 & 0 & 0 & 0 & 0 & 0 & A_{44} & 0 \\ 0 & 0 & 0 & 0 & 0 & 0 & 0 & A_{44} \end{bmatrix} \times \int_{-h/2}^{h/2} \begin{Bmatrix} \sigma_x \\ \sigma_y \\ \sigma_{xy} \\ \sigma_x z \\ \sigma_y z \\ \sigma_{xy} z \\ \sigma_{yz} \\ \sigma_{xz} \end{Bmatrix} dz \tag{6}$$

Let us use the fourth equation of FSDT in order to calculate w_s based on w_b:

$$\frac{\partial M_x}{\partial x} + \frac{\partial M_{xy}}{\partial y} - Q_x = 0 \tag{7}$$

Imposing equation (6) into equation (7), we have:

$$D_{11}\frac{\partial^3 w_b}{\partial x^3} + (D_{12} + D_{66})\frac{\partial^3 w_b}{\partial x \partial y^2} - A_{44}\frac{\partial w_s}{\partial x} = 0 \tag{8}$$

Integrating equation (8) based on x, ignoring the integral constants and then simplifying, the shear deflection is captured as:

$$w_s = W' = A\frac{\partial^2 w_b}{\partial x^2} + B\frac{\partial^2 w_b}{\partial y^2} \tag{9}$$

where A and B parameters are explained:

$$A = \frac{D_{11}}{A_{44}}, \ B = \frac{D_{12} + D_{66}}{A_{44}} \tag{10}$$

Then, the new shear deformation plate theory can be obtained as follows:

$$\text{Now: } w_b = w_0; \begin{Bmatrix} U(x, y, z, t) \\ V(x, y, z, t) \\ W(x, y, z, t) \end{Bmatrix} = \begin{Bmatrix} u(x, y, t) - z\dfrac{\partial w_0(x, y, t)}{\partial x} \\ v(x, y, t) - z\dfrac{\partial w_0(x, y, t)}{\partial y} \\ w_0(x, y, t) + A\dfrac{\partial^2 w_0(x, y, t)}{\partial x^2} + B\dfrac{\partial^2 w_0(x, y, t)}{\partial y^2} \end{Bmatrix} \tag{11}$$

Here, the potential energy of the plate (V) would be derived according to the Hamilton's principle as below [43]:

$$\delta V = \delta \int_0^t (S + \Omega - T)dt = 0 \tag{12}$$

where δS is the variation of strain energy and for the variation of kinetic energy δT has been allocated, and also δV is the variation of works done by external forces. The strain energy by kronecker delta would be calculated:

$$\delta S = \iiint_v (\sigma_{ij}\delta\varepsilon_{ij} - D_k\delta E_k - B_k\delta H_k)dV = 0 \tag{13}$$

In which the magnetic displacement and field are B_k and H_k, the electric displacement and field are D_k and E_k, and also the stress and strain tensors are σ_{ij} and ε_{ij}, respectively as follows [16–18, 37, 44, 45].

$$\sigma_{ij} = C_{ijkl}\varepsilon_{kl} - e_{kij}E_k - q_{kij}H_k \tag{14}$$

$$D_i = e_{ikl}\varepsilon_{kl} + \kappa_{ij}E_k + d_{ij}H_k \tag{15}$$

$$B_i = q_{ikl}\varepsilon_{kl} + d_{ij}E_k + \eta_{ij}H_k \tag{16}$$

In which κ_{ij} is the dielectric tensor, q_{kij} shows the piezomagnetic tensor, e_{kij} depicts the piezoelectric tensor, C_{ijkl} represents the elastic tensor and d_{ij} denotes the electro-magnetic tensor, respectively. These tensors are developed below:

$$\begin{Bmatrix} \varepsilon_{xx} \\ \varepsilon_{yy} \\ \gamma_{xz} \\ \gamma_{yz} \\ \gamma_{xy} \end{Bmatrix} = \begin{Bmatrix} \dfrac{\partial u}{\partial x} - z\dfrac{\partial^2 w_0}{\partial x^2} + \dfrac{1}{2}\left(A\dfrac{\partial^3 w_0}{\partial x^3} + B\dfrac{\partial^3 w_0}{\partial x\partial y^2} + \dfrac{\partial w_0}{\partial x}\right)^2 \\ \dfrac{\partial v}{\partial y} - z\dfrac{\partial^2 w_0}{\partial y^2} + \dfrac{1}{2}\left(A\dfrac{\partial^3 w_0}{\partial x^2\partial y} + B\dfrac{\partial^3 w_0}{\partial y^3} + \dfrac{\partial w_0}{\partial y}\right)^2 \\ A\dfrac{\partial^3 w_0}{\partial x^3} + B\dfrac{\partial^3 w_0}{\partial x\partial y^2} \\ A\dfrac{\partial^3 w_0}{\partial x^2\partial y} + B\dfrac{\partial^3 w_0}{\partial y^3} \\ \left(\dfrac{\partial u}{\partial y} + \dfrac{\partial v}{\partial x}\right) - 2z\dfrac{\partial^2 w_0}{\partial x\partial y} + \left(A\dfrac{\partial^3 w_0}{\partial x^3} + B\dfrac{\partial^3 w_0}{\partial x\partial y^2} + \dfrac{\partial w_0}{\partial x}\right)\left(A\dfrac{\partial^3 w_0}{\partial x^2\partial y} + B\dfrac{\partial^3 w_0}{\partial y^3} + \dfrac{\partial w_0}{\partial y}\right) \end{Bmatrix} \tag{17}$$

$$e_{kij} = \begin{bmatrix} 0 & 0 & \bar{e}_{31} \\ 0 & 0 & \bar{e}_{31} \\ \bar{e}_{15} & 0 & 0 \\ 0 & \bar{e}_{15} & 0 \\ 0 & 0 & 0 \end{bmatrix}, \ e_{ikl} = e_{kij}{}^T \tag{18}$$

$$q_{kij} = \begin{bmatrix} 0 & 0 & \bar{q}_{31} \\ 0 & 0 & \bar{q}_{31} \\ \bar{q}_{15} & 0 & 0 \\ 0 & \bar{q}_{15} & 0 \\ 0 & 0 & 0 \end{bmatrix}, \ q_{ikl} = q_{ikl}{}^T \tag{19}$$

$$
\begin{Bmatrix} \bar{e}_{31} \\ \bar{e}_{15} \\ \bar{\kappa}_{11} \\ \bar{\kappa}_{33} \\ \bar{q}_{31} \\ \bar{q}_{15} \\ \bar{d}_{11} \\ \bar{d}_{33} \\ \bar{\eta}_{11} \\ \bar{\eta}_{33} \end{Bmatrix} = \begin{Bmatrix} e_{31} - \dfrac{C_{13}e_{33}}{C_{33}} \\ e_{15} \\ \kappa_{11} \\ \kappa_{33} + \dfrac{e_{33}^2}{C_{33}} \\ q_{31} - \dfrac{C_{13}q_{33}}{C_{33}} \\ q_{15} \\ d_{11} \\ d_{33} + \dfrac{q_{33}e_{33}}{C_{33}} \\ \eta_{11} \\ \eta_{33} + \dfrac{q_{33}^2}{C_{33}} \end{Bmatrix} \tag{20}
$$

$$
\kappa_{ij} = \begin{bmatrix} \bar{\kappa}_{11} & 0 & 0 \\ 0 & \bar{\kappa}_{11} & 0 \\ 0 & 0 & \bar{\kappa}_{33} \end{bmatrix}, \quad d_{ij} = \begin{bmatrix} \bar{d}_{11} & 0 & 0 \\ 0 & \bar{d}_{11} & 0 \\ 0 & 0 & \bar{d}_{33} \end{bmatrix}, \quad \eta_{ij} = \begin{bmatrix} \bar{\eta}_{11} & 0 & 0 \\ 0 & \bar{\eta}_{11} & 0 \\ 0 & 0 & \bar{\eta}_{33} \end{bmatrix} \tag{21}
$$

In order to define the magnetic and electric potentials, the following linear relations were presented [16–18, 37, 44, 45].

$$
\overline{\Phi}(x, y, z) = -\cos\left(\frac{\pi z}{h}\right)\Phi(x, y) + \frac{2z\phi_0}{h} \tag{22}
$$

$$
\overline{\Psi}(x, y, z) = -\cos\left(\frac{\pi z}{h}\right)\Psi(x, y) + \frac{2z\psi_0}{h} \tag{23}
$$

In which $\Phi(x, y)$ and $\Psi(x, y)$ denote the electric and magnetic displacements and also ϕ_0 and ψ_0 represent electric and magnetic voltages, respectively. Afterwards, the electromagnetic field can be developed below:

$$
E_k = \begin{Bmatrix} \overline{E}_x \\ \overline{E}_y \\ \overline{E}_z \end{Bmatrix} = \begin{Bmatrix} -\dfrac{\partial \overline{\Phi}}{\partial x} \\ -\dfrac{\partial \overline{\Phi}}{\partial y} \\ -\dfrac{\partial \overline{\Phi}}{\partial z} \end{Bmatrix} = \begin{Bmatrix} \cos\left(\dfrac{\pi z}{h}\right)\dfrac{\partial \Phi}{\partial x} \\ \cos\left(\dfrac{\pi z}{h}\right)\dfrac{\partial \Phi}{\partial y} \\ -\dfrac{\pi}{h}\sin\left(\dfrac{\pi z}{h}\right)\Phi - \dfrac{2\phi_0}{h} \end{Bmatrix} \tag{24}
$$

$$
H_k = \begin{Bmatrix} \overline{H}_x \\ \overline{H}_y \\ \overline{H}_z \end{Bmatrix} = \begin{Bmatrix} -\dfrac{\partial \overline{\Psi}}{\partial x} \\ -\dfrac{\partial \overline{\Psi}}{\partial y} \\ -\dfrac{\partial \overline{\Psi}}{\partial z} \end{Bmatrix} = \begin{Bmatrix} \cos\left(\dfrac{\pi z}{h}\right)\dfrac{\partial \Psi}{\partial x} \\ \cos\left(\dfrac{\pi z}{h}\right)\dfrac{\partial \Psi}{\partial y} \\ -\dfrac{\pi}{h}\sin\left(\dfrac{\pi z}{h}\right)\Psi - \dfrac{2\psi_0}{h} \end{Bmatrix} \tag{25}
$$

The kinetic energy of the plate would be expressed [19, 20, 43]:

$$
T = \frac{1}{2}\int_A \int_{-h/2}^{h/2} \rho(z, T)\left(\left(\frac{\partial U}{\partial t}\right)^2 + \left(\frac{\partial V}{\partial t}\right)^2 + \left(\frac{\partial W}{\partial t}\right)^2\right)dzdA = 0 \tag{26}
$$

So the kinetic energy in variational form would be expanded as follows:

$$
\delta T = \int_A \int_{-h/2}^{h/2} \rho(z, T)\left[\left(-z^2\frac{\partial^4 w_0}{\partial x^2 \partial t^2} - z^2\frac{\partial^4 w_0}{\partial y^2 \partial t^2} - \frac{\partial^2 w_0}{\partial t^2} - A^2\frac{\partial^6 w_0}{\partial x^4 \partial t^2} - B^2\frac{\partial^6 w_0}{\partial y^4 \partial t^2} - 2A\frac{\partial^4 w_0}{\partial x^2 \partial t^2}\right.\right.
$$
$$
\left.\left. - 2B\frac{\partial^4 w_0}{\partial y^2 \partial t^2} - 2AB\frac{\partial^6 w_0}{\partial x^2 \partial y^2 \partial t^2}\right)\delta w_0\right]dzdA = 0 \tag{27}
$$

In which the mass moments of inertias are presented in the following:

$$(I_0, I_2) = \int_{-h/2}^{h/2} \rho(z, T)(1, z^2)\,dz \tag{28}$$

If $\delta V = 0$, then the nonlinear constitutive equations of motion can be obtained below:

$$
\begin{aligned}
\delta w_0 = 0; \; & -\frac{\partial^2 M_x}{\partial x^2} - \frac{\partial^2 M_y}{\partial y^2} - 2\frac{\partial^2 M_{xy}}{\partial x\partial y} + A\frac{\partial^3 Q_x}{\partial x^3} + B\frac{\partial^3 Q_x}{\partial x\partial y^2} + A\frac{\partial^3 Q_y}{\partial x^2\partial y} + B\frac{\partial^3 Q_y}{\partial y^3} \\
& + N_x\left(A^2\frac{\partial^6 w_0}{\partial x^6} + B^2\frac{\partial^6 w_0}{\partial x^2\partial y^4} + \frac{\partial^2 w_0}{\partial x^2} + 2AB\frac{\partial^6 w_0}{\partial x^4\partial y^2} + 2A\frac{\partial^4 w_0}{\partial x^4} + 2B\frac{\partial^4 w_0}{\partial x^2\partial y^2} \right) \\
& + N_y\left(A^2\frac{\partial^6 w_0}{\partial x^4\partial y^2} + B^2\frac{\partial^6 w_0}{\partial y^6} + \frac{\partial^2 w_0}{\partial y^2} + 2AB\frac{\partial^6 w_0}{\partial x^2\partial y^4} + 2A\frac{\partial^4 w_0}{\partial x^2\partial y^2} + 2B\frac{\partial^4 w_0}{\partial y^4} \right) \\
& + N_{xy}\left(2A^2\frac{\partial^6 w_0}{\partial x^5\partial y} + 4AB\frac{\partial^6 w_0}{\partial x^3\partial y^3} + 4A\frac{\partial^4 w_0}{\partial x^3\partial y} + 2B^2\frac{\partial^6 w_0}{\partial x\partial y^5} + 4B\frac{\partial^4 w_0}{\partial x\partial y^3} + 2\frac{\partial^2 w_0}{\partial x\partial y} \right) \\
& - I_2\left(\frac{\partial^4 w_0}{\partial x^2\partial t^2} + \frac{\partial^4 w_0}{\partial y^2\partial t^2} \right) - I_0\left(\frac{\partial^2 w_0}{\partial t^2} + A^2\frac{\partial^6 w_0}{\partial x^4\partial t^2} + B^2\frac{\partial^6 w_0}{\partial y^4\partial t^2} + 2A\frac{\partial^4 w_0}{\partial x^2\partial t^2} \right. \\
& \left. + 2B\frac{\partial^4 w_0}{\partial y^2\partial t^2} + 2AB\frac{\partial^6 w_0}{\partial x^2\partial y^2\partial t^2} \right) = q(x, y, t)
\end{aligned} \tag{29a}
$$

$$\delta\Phi = 0; \; \int_{-h/2}^{h/2}\left[\frac{\partial \overline{D}_x}{\partial x}\cos\left(\frac{\pi z}{h}\right) + \frac{\partial \overline{D}_y}{\partial y}\cos\left(\frac{\pi z}{h}\right) + \frac{\pi}{h}\overline{D}_z \sin\left(\frac{\pi z}{h}\right) \right] dz = 0 \tag{29b}$$

$$\delta\Psi = 0; \; \int_{-h/2}^{h/2}\left[\frac{\partial \overline{B}_x}{\partial x}\cos\left(\frac{\pi z}{h}\right) + \frac{\partial \overline{B}_y}{\partial y}\cos\left(\frac{\pi z}{h}\right) + \frac{\pi}{h}\overline{B}_z \sin\left(\frac{\pi z}{h}\right) \right] dz = 0 \tag{29c}$$

where N_i, M_i, and Q_i ($i = x, y, xy$) are nonlocal stress resultants, respectively. The $\overline{D}_i$ and $\overline{B}_i$ parameters in equation (29) are expanded below:

$$
\begin{Bmatrix} \overline{D}_x \\ \overline{D}_y \\ \overline{D}_z \end{Bmatrix} = \int_{-h/2}^{h/2} \begin{Bmatrix} D_x\cos\left(\frac{\pi z}{h}\right) \\ D_y\cos\left(\frac{\pi z}{h}\right) \\ D_z\frac{\pi}{h}\sin\left(\frac{\pi z}{h}\right) \end{Bmatrix} dz = \begin{Bmatrix} E_{15}\left(A\frac{\partial^3 w_0}{\partial x^3} + B\frac{\partial^3 w_0}{\partial x\partial y^2}\right) + X_{11}\frac{\partial\Phi}{\partial x} + Y_{11}\frac{\partial\Psi}{\partial x} \\ E_{15}\left(A\frac{\partial^3 w_0}{\partial x^2\partial y} + B\frac{\partial^3 w_0}{\partial y^3}\right) + X_{11}\frac{\partial\Phi}{\partial y} + Y_{11}\frac{\partial\Psi}{\partial y} \\ -E_{31}\frac{\partial^2 w_0}{\partial x^2} - E_{31}\frac{\partial^2 w_0}{\partial y^2} - X_{33}\Phi - Y_{33}\Psi \end{Bmatrix} \tag{30}
$$

$$
\begin{Bmatrix} \overline{B}_x \\ \overline{B}_y \\ \overline{B}_z \end{Bmatrix} = \int_{-h/2}^{h/2} \begin{Bmatrix} B_x\cos\left(\frac{\pi z}{h}\right) \\ B_y\cos\left(\frac{\pi z}{h}\right) \\ B_z\frac{\pi}{h}\sin\left(\frac{\pi z}{h}\right) \end{Bmatrix} dz = \begin{Bmatrix} F_{15}\left(A\frac{\partial^3 w_0}{\partial x^3} + B\frac{\partial^3 w_0}{\partial x\partial y^2}\right) + Y_{11}\frac{\partial\Phi}{\partial x} + Y_{22}\frac{\partial\Psi}{\partial x} \\ F_{15}\left(A\frac{\partial^3 w_0}{\partial x^2\partial y} + B\frac{\partial^3 w_0}{\partial y^3}\right) + Y_{11}\frac{\partial\Phi}{\partial y} + Y_{22}\frac{\partial\Psi}{\partial x} \\ -F_{31}\frac{\partial^2 w_0}{\partial x^2} - F_{31}\frac{\partial^2 w_0}{\partial y^2} - Y_{33}\Phi - Y_{44}\Psi \end{Bmatrix} \tag{31}
$$

The constants in equations (30), (31) can be exploded as follows:

$$
\begin{Bmatrix} E_{31} \\ E_{15} \\ X_{11} \\ X_{33} \end{Bmatrix} = \int_{-h/2}^{h/2} \begin{Bmatrix} \bar{e}_{31}\frac{\pi}{h}z\sin\left(\frac{\pi}{h}z\right) \\ \bar{e}_{15}\cos\left(\frac{\pi}{h}z\right) \\ \bar{\kappa}_{11}\cos^2\left(\frac{\pi}{h}z\right) \\ \bar{\kappa}_{33}\left(\frac{\pi}{h}\right)^2\sin^2\left(\frac{\pi}{h}z\right) \end{Bmatrix} dz \tag{32}
$$

$$\left\{ \begin{array}{c} Y_{11} \\ Y_{33} \end{array} \right\} = \int_{-h/2}^{h/2} \left\{ \begin{array}{c} \bar{d}_{11} \cos^2\left(\dfrac{\pi}{h}z\right) \\[2mm] \bar{d}_{33}\left(\dfrac{\pi}{h}\right)^2 \sin^2\left(\dfrac{\pi}{h}z\right) \end{array} \right\} dz \tag{33}$$

$$\left\{ \begin{array}{c} F_{31} \\ F_{15} \\ Y_{22} \\ Y_{44} \end{array} \right\} = \int_{-h/2}^{h/2} \left\{ \begin{array}{c} \bar{q}_{31} \dfrac{\pi}{h} z \sin\left(\dfrac{\pi}{h}z\right) \\[2mm] \bar{q}_{15} \cos\left(\dfrac{\pi}{h}z\right) \\[2mm] \bar{\eta}_{11} \cos^2\left(\dfrac{\pi}{h}z\right) \\[2mm] \bar{\eta}_{33}\left(\dfrac{\pi}{h}\right)^2 \sin^2\left(\dfrac{\pi}{h}z\right) \end{array} \right\} dz \tag{34}$$

The stiffness matrix for tension and flexure of the electromagnetic nanoplate are as follows:

$$A_{ij} = \int_{-\frac{h}{2}}^{\frac{h}{2}} \bar{C}_{ij}\, dz \quad (i, j = 1,\ 2,\ 4,\ 6), \quad D_{ij} = \int_{-\frac{h}{2}}^{\frac{h}{2}} \bar{C}_{ij} z^2\, dz \quad (i, j = 1,\ 2,\ 6) \tag{35}$$

$$\left\{ \begin{array}{c} \overline{C}_{11} \\ \overline{C}_{12} \\ \overline{C}_{44} \\ \overline{C}_{66} \end{array} \right\} = \left\{ \begin{array}{c} C_{11} - \dfrac{C_{13}^2}{C_{33}} \\[2mm] C_{12} - \dfrac{C_{13}^2}{C_{33}} \\[2mm] C_{44} \\ C_{66} \end{array} \right\} \tag{36}$$

Here, it is tried to explain the in-plane loads as below:

$$N^0 = [N_{ij}]^E + [N_{ij}]^{Mag} \tag{37}$$

In which N_{ij}^{Mag} and N_{ij}^E are the in-plane magnetic and electric forces as follows [16, 37, 44]:

$$N_x^E, N_y^E = \int_{-h/2}^{h/2} \bar{e}_{31} \frac{2\phi_0}{h} dz \tag{38a}$$

$$N_x^{Mag}, N_y^{Mag} = \int_{-h/2}^{h/2} \bar{q}_{31} \frac{2\psi_0}{h} dz \tag{38b}$$

2.2. Higher-order nonlocal strain gradient theory

According to this higher-order non-classical hypothesis the following equation is employed [46–48]:

$$(1 - \mu_1^2 \nabla^2)(1 - \mu_0^2 \nabla^2)\sigma_{ij} = C_{ijkl}(1 - \mu_1^2 \nabla^2)\varepsilon_{kl} - C_{ijkl} l^2 (1 - \mu_0^2 \nabla^2)\nabla^2 \varepsilon_{kl}; \quad \mu_0(nm) = e_0 a,$$

$$\mu_1(nm) = e_1 a, \quad \nabla^2 = \frac{\partial^2}{\partial x^2} + \frac{\partial^2}{\partial y^2} \tag{39}$$

where μ_0, μ_1, and l are lower and higher-order nonlocality parameters and strain gradient length scale constant, respectively. We can easily convert equation (39) into the other forms of size-dependent theories:

(a) Lower-order nonlocal strain gradient theory:

$$\left\{ \begin{array}{l} \mu_0 = e_0 a \\ \mu_1 = e_1 a \end{array} \right. \to \mu_0 = \mu_1 = \mu \to (1 - \mu^2 \nabla^2)\sigma_{ij} = C_{ijkl}(1 - l^2 \nabla^2)\varepsilon_{kl} \tag{40}$$

(b) Eringen's nonlocal elasticity theory:

$$\{ l = \mu_1 = 0 \to (1 - \mu_0^2 \nabla^2)\sigma_{ij} = C_{ijkl}\varepsilon_{kl} \tag{41}$$

(c) A model without stress nonlocality:

$$\{ \mu_0 = \mu_1 = 0 \to \sigma_{ij} = C_{ijkl}(1 - l^2 \nabla^2)\varepsilon_{kl} \tag{42}$$

By using higher-order nonlocal strain gradient theory and applying it on the stress resultants, we get:

$$(1 - \mu_1^2 \nabla^2)(1 - \mu_0^2 \nabla^2)\sigma_{ij} = C_{ijkl}(1 - \mu_1^2 \nabla^2)\varepsilon_{kl} - C_{ijkl}l^2(1 - \mu_0^2 \nabla^2)\nabla^2 \varepsilon_{kl} - e_{kij}E_k - q_{kij}H_k \tag{43a}$$

$$(1 - \mu_1^2 \nabla^2)(1 - \mu_0^2 \nabla^2)D_i = C_{ijkl}(1 - \mu_1^2 \nabla^2)\varepsilon_{kl} - C_{ijkl}l^2(1 - \mu_0^2 \nabla^2)\nabla^2 \varepsilon_{kl} + \kappa_{ij}E_k + d_{ij}H_k \tag{43b}$$

$$(1 - \mu_1^2 \nabla^2)(1 - \mu_0^2 \nabla^2)B_i = C_{ijkl}(1 - \mu_1^2 \nabla^2)\varepsilon_{kl} - C_{ijkl}l^2(1 - \mu_0^2 \nabla^2)\nabla^2 \varepsilon_{kl} + d_{ij}E_k + \eta_{ij}H_k \tag{43c}$$

The local forms of stress resultants were defined as follows:

$$(N_x, N_y, N_{xy}) = \int_{-h/2}^{h/2} (\sigma_x, \sigma_y, \sigma_{xy})dz \tag{44a}$$

$$(M_x, M_y, M_{xy}) = \int_{-h/2}^{h/2} (\sigma_x, \sigma_y, \sigma_{xy})z\,dz \tag{44b}$$

$$(Q_x, Q_y) = \int_{-h/2}^{h/2} (\sigma_{xz}, \sigma_{yz})dz \tag{44c}$$

Now, by substituting equation (17) into the equation (44) the stress resultants will be given in the form of equation below:

$$
\begin{bmatrix} N_{xx} \\ N_{yy} \\ N_{xy} \\ M_{xx} \\ M_{yy} \\ M_{xy} \\ Q_y \\ Q_x \end{bmatrix}^{Total} =
\begin{bmatrix}
A_{11} & A_{12} & 0 & 0 & 0 & 0 & 0 & 0 \\
A_{21} & A_{22} & 0 & 0 & 0 & 0 & 0 & 0 \\
0 & 0 & A_{66} & 0 & 0 & 0 & 0 & 0 \\
0 & 0 & 0 & D_{11} & D_{12} & 0 & 0 & 0 \\
0 & 0 & 0 & D_{21} & D_{22} & 0 & 0 & 0 \\
0 & 0 & 0 & 0 & 0 & D_{66} & 0 & 0 \\
0 & 0 & 0 & 0 & 0 & 0 & A_{44} & 0 \\
0 & 0 & 0 & 0 & 0 & 0 & 0 & A_{44}
\end{bmatrix}
$$

$$
\times
\begin{bmatrix}
\dfrac{\partial u}{\partial x} + \dfrac{1}{2}\left(A\dfrac{\partial^3 w_0}{\partial x^3} + B\dfrac{\partial^3 w_0}{\partial x \partial y^2} + \dfrac{\partial w_0}{\partial x}\right)^2 \\[2mm]
\dfrac{\partial v}{\partial y} + \dfrac{1}{2}\left(A\dfrac{\partial^3 w_0}{\partial x^2 \partial y} + B\dfrac{\partial^3 w_0}{\partial y^3} + \dfrac{\partial w_0}{\partial y}\right)^2 \\[2mm]
\left(\dfrac{\partial u}{\partial y} + \dfrac{\partial v}{\partial x}\right) + \left(A\dfrac{\partial^3 w_0}{\partial x^3} + B\dfrac{\partial^3 w_0}{\partial x \partial y^2} + \dfrac{\partial w_0}{\partial x}\right)\left(A\dfrac{\partial^3 w_0}{\partial x^2 \partial y} + B\dfrac{\partial^3 w_0}{\partial y^3} + \dfrac{\partial w_0}{\partial y}\right) \\[2mm]
-\dfrac{\partial^2 w_0}{\partial x^2} \\[2mm]
-\dfrac{\partial^2 w_0}{\partial y^2} \\[2mm]
-\dfrac{\partial^2 w_0}{\partial x \partial y} \\[2mm]
A\dfrac{\partial^3 w_0}{\partial x^2 \partial y} + B\dfrac{\partial^3 w_0}{\partial y^3} \\[2mm]
A\dfrac{\partial^3 w_0}{\partial x^3} + B\dfrac{\partial^3 w_0}{\partial x \partial y^2}
\end{bmatrix}^{Mech}
$$

$$
+ \begin{Bmatrix} 2\bar{e}_{31}\phi_0 \\ 2\bar{e}_{31}\phi_0 \\ 0 \\ E_{31}\Phi \\ E_{31}\Phi \\ 0 \\ -E_{15}\dfrac{\partial \Phi}{\partial y} \\ -E_{15}\dfrac{\partial \Phi}{\partial x} \end{Bmatrix}^{Electrical}
+ \begin{Bmatrix} 2\bar{q}_{31}\psi_0 \\ 2\bar{q}_{31}\psi_0 \\ 0 \\ F_{31}\Psi \\ F_{31}\Psi \\ 0 \\ -F_{15}\dfrac{\partial \Psi}{\partial y} \\ -F_{15}\dfrac{\partial \Psi}{\partial x} \end{Bmatrix}^{Magnetic}
\tag{45}
$$

Then, equation (45) can be employed to re-formulate the stress resultants which will lead to the forms as follows:

$$(1 - (\mu_0^2 + \mu_1^2)\nabla^2 + \mu_0^2\mu_1^2\nabla^4)M_x = -[(1 - \mu_1^2\nabla^2) - l^2(1 - \mu_0^2\nabla^2)\nabla^2]\left(D_{11}\frac{\partial^2 w_0}{\partial x^2} + D_{12}\frac{\partial^2 w_0}{\partial y^2}\right) \quad (46a)$$

$$(1 - (\mu_0^2 + \mu_1^2)\nabla^2 + \mu_0^2\mu_1^2\nabla^4)M_y = -[(1 - \mu_1^2\nabla^2) - l^2(1 - \mu_0^2\nabla^2)\nabla^2]\left(D_{21}\frac{\partial^2 w_0}{\partial x^2} + D_{22}\frac{\partial^2 w_0}{\partial y^2}\right) \quad (46b)$$

$$(1 - (\mu_0^2 + \mu_1^2)\nabla^2 + \mu_0^2\mu_1^2\nabla^4)M_{xy} = -[(1 - \mu_1^2\nabla^2) - l^2(1 - \mu_0^2\nabla^2)\nabla^2]\left(D_{66}\frac{\partial^2 w_0}{\partial x\partial y}\right) \quad (46c)$$

$$(1 - (\mu_0^2 + \mu_1^2)\nabla^2 + \mu_0^2\mu_1^2\nabla^4)Q_x = [(1 - \mu_1^2\nabla^2) - l^2(1 - \mu_0^2\nabla^2)\nabla^2]A_{44}\left(A\frac{\partial^3 w_0}{\partial x^3} + B\frac{\partial^3 w_0}{\partial x\partial y^2}\right) \quad (46d)$$

$$(1 - (\mu_0^2 + \mu_1^2)\nabla^2 + \mu_0^2\mu_1^2\nabla^4)Q_y = [(1 - \mu_1^2\nabla^2) - l^2(1 - \mu_0^2\nabla^2)\nabla^2]A_{44}\left(A\frac{\partial^3 w_0}{\partial x^2\partial y} + B\frac{\partial^3 w_0}{\partial y^3}\right) \quad (46e)$$

$$(1 - (\mu_0^2 + \mu_1^2)\nabla^2 + \mu_0^2\mu_1^2\nabla^4)\begin{Bmatrix}\overline{D}_x \\ \overline{D}_y \\ \overline{D}_z\end{Bmatrix}$$

$$= \begin{Bmatrix} [(1 - \mu_1^2\nabla^2) - l^2(1 - \mu_0^2\nabla^2)\nabla^2]E_{15}\left(A\frac{\partial^3 w_0}{\partial x^3} + B\frac{\partial^3 w_0}{\partial x\partial y^2}\right) + X_{11}\frac{\partial\Phi}{\partial x} + Y_{11}\frac{\partial\Psi}{\partial x} \\ [(1 - \mu_1^2\nabla^2) - l^2(1 - \mu_0^2\nabla^2)\nabla^2]E_{15}\left(A\frac{\partial^3 w_0}{\partial x^2\partial y} + B\frac{\partial^3 w_0}{\partial y^3}\right) + X_{11}\frac{\partial\Phi}{\partial y} + Y_{11}\frac{\partial\Psi}{\partial y} \\ -[(1 - \mu_1^2\nabla^2) - l^2(1 - \mu_0^2\nabla^2)\nabla^2]\left(E_{31}\frac{\partial^2 w_0}{\partial x^2} + E_{31}\frac{\partial^2 w_0}{\partial y^2}\right) - X_{33}\Phi - Y_{33}\Psi \end{Bmatrix} \quad (47)$$

$$(1 - (\mu_0^2 + \mu_1^2)\nabla^2 + \mu_0^2\mu_1^2\nabla^4)\begin{Bmatrix}\overline{B}_x \\ \overline{B}_y \\ \overline{B}_z\end{Bmatrix}$$

$$= \begin{Bmatrix} [(1 - \mu_1^2\nabla^2) - l^2(1 - \mu_0^2\nabla^2)\nabla^2]F_{15}\left(A\frac{\partial^3 w_0}{\partial x^3} + B\frac{\partial^3 w_0}{\partial x\partial y^2}\right) + Y_{11}\frac{\partial\Phi}{\partial x} + Y_{22}\frac{\partial\Psi}{\partial x} \\ [(1 - \mu_1^2\nabla^2) - l^2(1 - \mu_0^2\nabla^2)\nabla^2]F_{15}\left(A\frac{\partial^3 w_0}{\partial x^2\partial y} + B\frac{\partial^3 w_0}{\partial y^3}\right) + Y_{11}\frac{\partial\Phi}{\partial y} + Y_{22}\frac{\partial\Psi}{\partial x} \\ -[(1 - \mu_1^2\nabla^2) - l^2(1 - \mu_0^2\nabla^2)\nabla^2]\left(F_{31}\frac{\partial^2 w_0}{\partial x^2} + F_{31}\frac{\partial^2 w_0}{\partial y^2}\right) - Y_{33}\Phi - Y_{44}\Psi \end{Bmatrix} \quad (48)$$

Eventually, by assembling equations (46)–(48) and using equation (38) and inserting them into equation (29), the electromagnetic forced vibrations equations will be acquired.

3. Analytical approach

To solve the vibrational equations of the nanoplate with four sides of the simply-supported, the Navier solution method is used. In the case of Navier approach, the displacement functions are considered as Fourier series expansion, in addition to satisfying the equations, the boundary conditions of the nanoplate with fully simply-supported are also satisfied [20]:

$$\begin{Bmatrix} w_0(x, y, t) \\ \Phi(x, y, t) \\ \Psi(x, y, t) \end{Bmatrix} = \begin{Bmatrix} \displaystyle\sum_{m=1}^{\infty}\sum_{n=1}^{\infty} W_{0mn} \\ \displaystyle\sum_{m=1}^{\infty}\sum_{n=1}^{\infty} \Phi_{0mn} \\ \displaystyle\sum_{m=1}^{\infty}\sum_{n=1}^{\infty} \Psi_{0mn} \end{Bmatrix} \times \sin(\omega_n t) \times \sin\left(\frac{m\pi}{L_x}x\right)\sin\left(\frac{n\pi}{L_y}y\right) \quad (49)$$

In which W_{0mn}, Φ_{0mn}, and Ψ_{0mn} represent the displacement and potentials unknown variables, m and n denote the half-wave numbers and ω_n shows the natural frequency related to intrinsic properties of the system such as mass and stiffness. The dynamic load is distributed uniformly and harmonically on the nanoplate that was showed in figure 1(b) and is taken in the form of the following expression [19]:

$$q(x, y, t) = \sum_{n=1}^{\infty} \sum_{m=1}^{\infty} q_m \sin(\omega_{ex} t) \times \sin\left(\frac{m\pi}{L_x}x\right) \sin\left(\frac{n\pi}{L_y}y\right) \tag{50a}$$

$$q_m = \frac{4q_0}{mn} \int_{y_0-c_2/2}^{y_0+c_2/2} \int_{x_0-c_1/2}^{x_0+c_1/2} \sin\left(\frac{m\pi}{L_x}x\right) \sin\left(\frac{n\pi}{L_y}y\right) dxdy$$

$$= \frac{16q_0}{mn\pi^2} \sin\left(\frac{m\pi}{L_x}x_0\right) \sin\left(\frac{m\pi}{L_x}\frac{c_1}{2}\right) \sin\left(\frac{n\pi}{L_y}y_0\right) \sin\left(\frac{n\pi}{L_y}\frac{c_2}{2}\right) \tag{50b}$$

In which q_m is the Fourier coefficient, q_0 is the uniform load amplitude and ω_{ex} is the excitation frequency, respectively. By substituting equation (50) into the equations of motion, the algebraic equations can be obtained:

$$\left(\begin{bmatrix} k_{11} & k_{12} & k_{13} \\ k_{21} & k_{22} & k_{23} \\ k_{31} & k_{32} & k_{33} \end{bmatrix} - \omega_n^2 \begin{bmatrix} m_{11} & m_{12} & m_{13} \\ m_{21} & m_{22} & m_{23} \\ m_{31} & m_{32} & m_{33} \end{bmatrix}\right) \begin{Bmatrix} W_{0mn} \\ \Phi_{0mn} \\ \Psi_{0mn} \end{Bmatrix} = \begin{Bmatrix} 0 \\ 0 \\ 0 \end{Bmatrix} \tag{51}$$

$$\left(\begin{bmatrix} k_{11} & k_{12} & k_{13} \\ k_{21} & k_{22} & k_{23} \\ k_{31} & k_{32} & k_{33} \end{bmatrix} - \Delta r^2 \begin{bmatrix} m_{11} & m_{12} & m_{13} \\ m_{21} & m_{22} & m_{23} \\ m_{31} & m_{32} & m_{33} \end{bmatrix}\right) \begin{Bmatrix} W_{0mn} \\ \Phi_{0mn} \\ \Psi_{0mn} \end{Bmatrix}$$
$$= \begin{Bmatrix} (1 - (\mu_0^2 + \mu_1^2)\nabla^2 + \mu_0^2\mu_1^2\nabla^4)q(x, y, t) \\ 0 \\ 0 \end{Bmatrix} \tag{52a}$$

$$\Delta r = \frac{\omega_{ex}}{\omega_n} \tag{52b}$$

where Δr is the excitation to natural frequency ratio. The stiffness matrix is k_{ij} ($i, j = 1, 2, 3$) and m_{ij} ($i, j = 1, 2, 3$) denotes the mass matrix extracted in the following:

$$k_{11} = \left\{\left[-D_{11}\frac{\partial^4}{\partial x^4} - 2(D_{12} + D_{66})\frac{\partial^4}{\partial x^2\partial y^2} - D_{22}\frac{\partial^4}{\partial y^4} + D_{11}\left(A\frac{\partial^6}{\partial x^6} + B\frac{\partial^6}{\partial x^4\partial y^2}\right) + (D_{12} + D_{66})\right.\right.$$

$$\times \left(A\frac{\partial^6}{\partial x^2\partial y^4} + B\frac{\partial^6}{\partial y^6}\right) + (D_{11} + D_{12} + D_{66})\left(A\frac{\partial^6}{\partial x^4\partial y^2} + B\frac{\partial^6}{\partial x^2\partial y^4}\right)\bigg] - (\mu_1^2 + l^2)\bigg[D_{11}\frac{\partial^6}{\partial x^6}$$

$$+ 2(D_{12} + D_{66})\frac{\partial^6}{\partial x^4\partial y^2} + D_{22}\frac{\partial^6}{\partial x^2\partial y^4} + D_{11}\left(A\frac{\partial^8}{\partial x^8} + B\frac{\partial^8}{\partial x^6\partial y^2}\right) + (D_{12} + D_{66})\left(A\frac{\partial^8}{\partial x^4\partial y^4}\right.$$

$$\left. + B\frac{\partial^8}{\partial x^2\partial y^6}\right) + (D_{11} + D_{12} + D_{66})\left(A\frac{\partial^8}{\partial x^6\partial y^2} + B\frac{\partial^8}{\partial x^4\partial y^4}\right)\bigg] - (\mu_1^2 + l^2)\bigg[D_{11}\frac{\partial^6}{\partial x^4\partial y^2}$$

$$+ 2(D_{12} + D_{66})\frac{\partial^6}{\partial x^2\partial y^4} + D_{22}\frac{\partial^6}{\partial y^6} + D_{11}\left(A\frac{\partial^8}{\partial x^6\partial y^2} + B\frac{\partial^8}{\partial x^4\partial y^4}\right) + (D_{12} + D_{66})$$

$$\times \left(A\frac{\partial^8}{\partial x^2\partial y^6} + B\frac{\partial^8}{\partial y^8}\right) + (D_{11} + D_{12} + D_{66})\left(A\frac{\partial^8}{\partial x^4\partial y^4} + B\frac{\partial^8}{\partial x^2\partial y^6}\right)\bigg] + l^2\mu_0^2\bigg[D_{11}\frac{\partial^8}{\partial x^8}$$

$$+ 2(D_{12} + D_{66})\frac{\partial^8}{\partial x^6\partial y^2} + D_{22}\frac{\partial^8}{\partial x^4\partial y^4} + D_{11}\left(A\frac{\partial^{10}}{\partial x^{10}} + B\frac{\partial^{10}}{\partial x^8\partial y^2}\right) + (D_{12} + D_{66})\left(A\frac{\partial^{10}}{\partial x^6\partial y^4}\right.$$

$$\left. + B\frac{\partial^{10}}{\partial x^4\partial y^6}\right) + (D_{11} + D_{12} + D_{66})\left(A\frac{\partial^{10}}{\partial x^8\partial y^2} + B\frac{\partial^{10}}{\partial x^6\partial y^4}\right)\bigg] + l^2\mu_0^2\bigg[D_{11}\frac{\partial^8}{\partial x^4\partial y^4} + 2(D_{12} + D_{66})$$

$$\times \frac{\partial^8}{\partial x^2\partial y^6} + D_{22}\frac{\partial^8}{\partial y^8} + D_{11}\left(A\frac{\partial^{10}}{\partial x^6\partial y^4} + B\frac{\partial^{10}}{\partial x^4\partial y^6}\right) + (D_{12} + D_{66}) \times \left(A\frac{\partial^{10}}{\partial x^2\partial y^8} + B\frac{\partial^{10}}{\partial y^{10}}\right)$$

$$+ (D_{11} + D_{12} + D_{66})\left(A\frac{\partial^{10}}{\partial x^4\partial y^6} + B\frac{\partial^{10}}{\partial x^2\partial y^8}\right)\bigg] + 2l^2\mu_0^2\bigg[D_{11}\frac{\partial^8}{\partial x^6\partial y^2} + 2(D_{12} + D_{66})\frac{\partial^8}{\partial x^4\partial y^4}$$

$$+ D_{22}\frac{\partial^8}{\partial x^2\partial y^6} + D_{11}\left(A\frac{\partial^{10}}{\partial x^8\partial y^2} + B\frac{\partial^{10}}{\partial x^6\partial y^4}\right) + (D_{12} + D_{66})\left(A\frac{\partial^{10}}{\partial x^4\partial y^6} + B\frac{\partial^{10}}{\partial x^2\partial y^8}\right)$$

$$+ (D_{11} + D_{12} + D_{66})\left(A\frac{\partial^{10}}{\partial x^6\partial y^4} + B\frac{\partial^{10}}{\partial x^4\partial y^6}\right)\bigg]\bigg\} + N^0 \times \left(A^2\frac{\partial^6}{\partial x^6} + (B^2 + 2AB)\frac{\partial^6}{\partial x^2\partial y^4} + \nabla^2\right.$$

$$+ (2AB + A^2)\frac{\partial^6}{\partial x^4 \partial y^2} + 2A\frac{\partial^4}{\partial x^4} + 2(A + B)\frac{\partial^4}{\partial x^2 \partial y^2} + B^2\frac{\partial^6}{\partial y^6} + 2B\frac{\partial^4}{\partial y^4}\Bigg) - N^0(\mu_0^2 + \mu_1^2)$$

$$\times \Bigg(A^2\frac{\partial^8}{\partial x^8} + (B^2 + 2AB)\frac{\partial^8}{\partial x^4 \partial y^4} + \frac{\partial^4}{\partial x^4} + \frac{\partial^4}{\partial x^2 \partial y^2} + (2AB + A^2)\frac{\partial^8}{\partial x^6 \partial y^2} + 2A\frac{\partial^6}{\partial x^6}$$

$$+ 2(A + B)\frac{\partial^6}{\partial x^4 \partial y^2} + B^2\frac{\partial^8}{\partial x^2 \partial y^6} + 2B\frac{\partial^6}{\partial x^2 \partial y^4}\Bigg) - N^0(\mu_0^2 + \mu_1^2)\Bigg(A^2\frac{\partial^8}{\partial x^6 \partial y^2} + (B^2 + 2AB)$$

$$\times \frac{\partial^8}{\partial x^2 \partial y^6} + \frac{\partial^4}{\partial x^2 \partial y^2} + \frac{\partial^4}{\partial y^4} + (2AB + A^2)\frac{\partial^8}{\partial x^4 \partial y^4} + 2A\frac{\partial^6}{\partial x^4 \partial y^2} + 2(A + B)\frac{\partial^6}{\partial x^2 \partial y^4}$$

$$+ B^2\frac{\partial^8}{\partial y^8} + 2B\frac{\partial^6}{\partial y^6}\Bigg) + N^0\mu_0^2\mu_1^2\Bigg(A^2\frac{\partial^{10}}{\partial x^{10}} + (B^2 + 2AB)\frac{\partial^{10}}{\partial x^6 \partial y^4} + \frac{\partial^6}{\partial x^6} + \frac{\partial^6}{\partial x^4 \partial y^2}$$

$$+ (2AB + A^2)\frac{\partial^{10}}{\partial x^8 \partial y^2} + 2A\frac{\partial^8}{\partial x^8} + 2(A + B)\frac{\partial^8}{\partial x^6 \partial y^2} + B^2\frac{\partial^{10}}{\partial x^4 \partial y^6} + 2B\frac{\partial^8}{\partial x^4 \partial y^4}\Bigg)$$

$$+ N^0\mu_0^2\mu_1^2\Bigg(A^2\frac{\partial^{10}}{\partial x^6 \partial y^4} + (B^2 + 2AB)\frac{\partial^{10}}{\partial x^2 \partial y^8} + \frac{\partial^6}{\partial x^2 \partial y^4} + \frac{\partial^6}{\partial y^6} + (2AB + A^2)\frac{\partial^{10}}{\partial x^4 \partial y^6}$$

$$+ 2A\frac{\partial^8}{\partial x^4 \partial y^4} + 2(A + B)\frac{\partial^8}{\partial x^2 \partial y^6} + B^2\frac{\partial^{10}}{\partial y^{10}} + 2B\frac{\partial^8}{\partial y^8}\Bigg) + 2N^0\mu_0^2\mu_1^2\Bigg(A^2\frac{\partial^{10}}{\partial x^8 \partial y^2}$$

$$+ (B^2 + 2AB)\frac{\partial^{10}}{\partial x^4 \partial y^6} + \frac{\partial^6}{\partial x^4 \partial y^2} + \frac{\partial^6}{\partial x^2 \partial y^4} + (2AB + A^2)\frac{\partial^{10}}{\partial x^6 \partial y^4}$$

$$+ 2A\frac{\partial^8}{\partial x^6 \partial y^2} + 2(A + B)\frac{\partial^8}{\partial x^4 \partial y^4} + B^2\frac{\partial^{10}}{\partial x^2 \partial y^8} + 2B\frac{\partial^8}{\partial x^2 \partial y^6}\Bigg)\Bigg\}$$

$$\times \sin(\omega_n t) \times \sin\left(\frac{m\pi}{L_x}x\right)\sin\left(\frac{n\pi}{L_y}y\right)$$

$$k_{12} = -\Bigg[E_{15}\Bigg(A\frac{\partial^4}{\partial x^4} + B\frac{\partial^4}{\partial y^4} + (A + B)\frac{\partial^4}{\partial x^2 \partial y^2}\Bigg) - E_{31}\Bigg(\frac{\partial^2}{\partial x^2} + \frac{\partial^2}{\partial y^2}\Bigg)\Bigg] \times \sin(\omega_n t)$$

$$\times \sin\left(\frac{m\pi}{L_x}x\right)\sin\left(\frac{n\pi}{L_y}y\right)$$

$$k_{13} = -\Bigg[F_{15}\Bigg(A\frac{\partial^4}{\partial x^4} + B\frac{\partial^4}{\partial y^4} + (A + B)\frac{\partial^4}{\partial x^2 \partial y^2}\Bigg) - F_{31}\Bigg(\frac{\partial^2}{\partial x^2} + \frac{\partial^2}{\partial y^2}\Bigg)\Bigg] \times \sin(\omega_n t)$$

$$\times \sin\left(\frac{m\pi}{L_x}x\right)\sin\left(\frac{n\pi}{L_y}y\right)$$

$$k_{21} = \Bigg[E_{15}\Bigg(A\frac{\partial^4}{\partial x^4} + B\frac{\partial^4}{\partial y^4} + (A + B)\frac{\partial^4}{\partial x^2 \partial y^2}\Bigg) - E_{31}\Bigg(\frac{\partial^2}{\partial x^2} + \frac{\partial^2}{\partial y^2}\Bigg)\Bigg] \times \sin(\omega_n t)$$

$$\times \sin\left(\frac{m\pi}{L_x}x\right)\sin\left(\frac{n\pi}{L_y}y\right)$$

$$k_{22} = \Bigg[X_{11}\Bigg(\frac{\partial^2}{\partial x^2} + \frac{\partial^2}{\partial y^2}\Bigg) - X_{33}\Bigg] \times \sin(\omega_n t) \times \sin\left(\frac{m\pi}{L_x}x\right)\sin\left(\frac{n\pi}{L_y}y\right)$$

$$k_{23} = \Bigg[Y_{11}\Bigg(\frac{\partial^2}{\partial x^2} + \frac{\partial^2}{\partial y^2}\Bigg) - Y_{33}\Bigg] \times \sin(\omega_n t) \times \sin\left(\frac{m\pi}{L_x}x\right)\sin\left(\frac{n\pi}{L_y}y\right)$$

$$k_{31} = \Bigg[F_{15}\Bigg(A\frac{\partial^4}{\partial x^4} + B\frac{\partial^4}{\partial y^4} + (A + B)\frac{\partial^4}{\partial x^2 \partial y^2}\Bigg) - F_{31}\Bigg(\frac{\partial^2}{\partial x^2} + \frac{\partial^2}{\partial y^2}\Bigg)\Bigg] \times \sin(\omega_n t)$$

$$\times \sin\left(\frac{m\pi}{L_x}x\right)\sin\left(\frac{n\pi}{L_y}y\right)$$

$$k_{32} = \Bigg[Y_{11}\Bigg(\frac{\partial^2}{\partial x^2} + \frac{\partial^2}{\partial y^2}\Bigg) - Y_{33}\Bigg] \times \sin(\omega_n t) \times \sin\left(\frac{m\pi}{L_x}x\right)\sin\left(\frac{n\pi}{L_y}y\right)$$

$$k_{33} = \Bigg[Y_{22}\Bigg(\frac{\partial^2}{\partial x^2} + \frac{\partial^2}{\partial y^2}\Bigg) - Y_{44}\Bigg] \times \sin(\omega_n t) \times \sin\left(\frac{m\pi}{L_x}x\right)\sin\left(\frac{n\pi}{L_y}y\right)$$

$$
\begin{aligned}
m_{11} = \Bigg\{ &-I_2\left(\frac{\partial^4}{\partial x^2 \partial t^2} + \frac{\partial^4}{\partial y^2 \partial t^2}\right) - I_0\Bigg(\frac{\partial^2}{\partial t^2} + A^2\frac{\partial^6}{\partial x^4 \partial t^2} + B^2\frac{\partial^6}{\partial y^4 \partial t^2} + 2A\frac{\partial^4}{\partial x^2 \partial t^2} + 2B\frac{\partial^4}{\partial y^2 \partial t^2} \\
&+ 2AB\frac{\partial^6}{\partial x^2 \partial y^2 \partial t^2}\Bigg) - (\mu_0^2 + \mu_1^2)\Bigg(-I_2\left(\frac{\partial^6}{\partial x^4 \partial t^2} + \frac{\partial^6}{\partial x^2 \partial y^2 \partial t^2}\right) - I_0\Bigg(\frac{\partial^4}{\partial x^2 \partial t^2} + A^2\frac{\partial^8}{\partial x^6 \partial t^2} \\
&+ B^2\frac{\partial^8}{\partial x^2 \partial y^4 \partial t^2} + 2A\frac{\partial^6}{\partial x^4 \partial t^2} + 2B\frac{\partial^6}{\partial x^2 \partial y^2 \partial t^2} + 2AB\frac{\partial^8}{\partial x^4 \partial y^2 \partial t^2}\Bigg)\Bigg) - (\mu_0^2 + \mu_1^2) \\
\times &\Bigg(-I_2\left(\frac{\partial^6}{\partial x^2 \partial y^2 \partial t^2} + \frac{\partial^6}{\partial y^4 \partial t^2}\right) - I_0\Bigg(\frac{\partial^4}{\partial y^2 \partial t^2} + A^2\frac{\partial^8}{\partial x^4 \partial y^2 \partial t^2} + B^2\frac{\partial^8}{\partial y^6 \partial t^2} \\
&+ 2A\frac{\partial^6}{\partial x^2 \partial y^2 \partial t^2} + 2B\frac{\partial^6}{\partial y^4 \partial t^2} + 2AB\frac{\partial^8}{\partial x^2 \partial y^4 \partial t^2}\Bigg)\Bigg) + \mu_0^2\mu_1^2\Bigg(-I_2\left(\frac{\partial^8}{\partial x^6 \partial t^2} + \frac{\partial^8}{\partial x^4 \partial y^2 \partial t^2}\right) \\
&- I_0\Bigg(\frac{\partial^6}{\partial x^4 \partial t^2} + A^2\frac{\partial^{10}}{\partial x^8 \partial t^2} + B^2\frac{\partial^{10}}{\partial x^4 \partial y^4 \partial t^2} + 2A\frac{\partial^8}{\partial x^6 \partial t^2} + 2B\frac{\partial^8}{\partial x^4 \partial y^2 \partial t^2} \\
&+ 2AB\frac{\partial^{10}}{\partial x^6 \partial y^2 \partial t^2}\Bigg)\Bigg) + \mu_0^2\mu_1^2\Bigg(-I_2\left(\frac{\partial^8}{\partial x^2 \partial y^4 \partial t^2} + \frac{\partial^{10}}{\partial y^6 \partial t^2}\right) - I_0\Bigg(\frac{\partial^6}{\partial y^4 \partial t^2} \\
&+ A^2\frac{\partial^{10}}{\partial x^4 \partial y^4 \partial t^2} + B^2\frac{\partial^{10}}{\partial y^8 \partial t^2} + 2A\frac{\partial^8}{\partial x^2 \partial y^4 \partial t^2} + 2B\frac{\partial^8}{\partial y^6 \partial t^2} + 2AB\frac{\partial^{10}}{\partial x^2 \partial y^6 \partial t^2}\Bigg)\Bigg) \\
&2\mu_0^2\mu_1^2\Bigg(-I_2\left(\frac{\partial^8}{\partial x^4 \partial y^2 \partial t^2} + \frac{\partial^8}{\partial x^2 \partial y^4 \partial t^2}\right) - I_0\Bigg(\frac{\partial^6}{\partial x^2 \partial y^2 \partial t^2} + A^2\frac{\partial^8}{\partial x^6 \partial y^2 \partial t^2} + B^2\frac{\partial^{10}}{\partial x^2 \partial y^6 \partial t^2} \\
&+ 2A\frac{\partial^8}{\partial x^4 \partial y^2 \partial t^2} + 2B\frac{\partial^8}{\partial x^2 \partial y^4 \partial t^2} + 2AB\frac{\partial^{10}}{\partial x^4 \partial y^4 \partial t^2}\Bigg)\Bigg)\Bigg\} \times \sin(\omega_n t) \times \sin\left(\frac{m\pi}{L_x}x\right)\sin\left(\frac{n\pi}{L_y}y\right)
\end{aligned}
$$

$$m_{12} = m_{13} = m_{21} = m_{22} = m_{23} = m_{31} = m_{32} = m_{33} = 0$$

To obtain the natural frequencies, the determinant of the coefficient matrix should be set to zero. After calculating natural frequencies, we can solve the linear algebraic equations of motion in order to calculate maximum dynamic deflections by the help of many simple methods. In this paper, the general Cramer's explicit rule is used as below:

$$[K]\{x\} = \{q\} \tag{53}$$

$$
\begin{aligned}
1 \leqslant i_1 < i_2 < \ldots < i_k \leqslant n \\
1 \leqslant j_1 < j_2 < \ldots < j_k \leqslant m
\end{aligned} \tag{54}
$$

Let $x_{I,J}$ be the $k \times k$ submatrix of x with rows and columns in:

$$
\begin{aligned}
I: &= (i_1, \ldots, i_k) \\
J: &= (j_1, \ldots, j_k)
\end{aligned} \tag{55}
$$

Let $K_q = (I, J)$ be the $n \times n$ matrix formed by replacing the i_s column of K by the j_s column of q, for all $s = 1,\ldots, k$. Then:

$$\det x_{I,J} = \frac{\det(K_q(I, J))}{\det(K)} \tag{56}$$

$$
K = \begin{bmatrix} k_{11} - \Delta r^2 m_{11} & k_{12} & k_{13} \\ k_{21} & k_{22} & k_{23} \\ k_{31} & k_{32} & k_{33} \end{bmatrix}; \quad x_j = (W_{0mn}, \ \Phi_{0mn}, \ \Psi_{0mn})^T; \quad q = (q(t), \ 0, \ 0)^T \tag{57}
$$

4. Numerical results and discussions

Initially, in order to validate the results which are developed from the new first-order shear deformation theory (OVFSDT) this comparison section should be presented within which several well-known references are investigated. In the first glance, table 1 will show the results of [49–51] which are compared with the present formulation in which molecular dynamic simulation (MD) and also first-order shear deformation theory (FSDT) were applied. It is worth noting that with enlarging the dimensions of the nanoplate the results of the OVFSDT inclined to the MD results. Principally, table 1 represents that the results of the OVFSDT are in an excellent agreement with other methods. To further validate the present OVFSDT, table 2 is documented. This

Table 1. Results of critical biaxial buckling loads for a square nanoplate obtained from the present theory and [52]. $E = 1$ TPa, $\upsilon = 0.16$, $k_s = 5/6$, $\mu = 1.81$ nm^2, *SSSS*. Reprinted from [52], Copyright (2018), with permission from Elsevier.

The critical buckling load of a biaxially loaded nanoplate (nN nm^{-1})				
OVFSDT	FSDT-DQM [49]	FSDT-DQM [50]	MD results [51]	Lx = Ly (nm)
1.0274	1.0749	1.0809	1.0837	4.99
0.621 51	0.6523	0.6519	0.6536	8.080
0.438 32	0.4356	0.4350	0.4331	10.77
0.261 22	0.2645	0.2639	0.2609	14.65
0.170 75	0.1751	0.1748	0.1714	18.51
0.119 63	0.1239	0.1237	0.1191	22.35
0.088 56	0.0917	0.0914	0.0889	26.22
0.069 18	0.0707	0.0705	0.0691	30.04
0.055 68	0.0561	0.0560	0.0554	33.85
0.044 88	0.0453	0.0451	0.0449	37.81

Table 2. Results of critical biaxial buckling loads for a rectangular nanoplate obtained from the present theory and [52]. $E = 1$ TPa, $\upsilon = 0.16$, $k_s = 5/6$, $\mu = 1.81$ nm^2, *SSSS*. Reprinted from [52], Copyright (2018), with permission from Elsevier.

The critical buckling load of a biaxially loaded nanoplate (nN nm^{-1})			
OVFSDT	FSDT [50]	MD results [51]	Lx/Ly
0.524 49	0.5115	0.5101	0.5
0.562 23	0.5715	0.5693	0.75
0.642 25	0.6622	0.6595	1.25
0.755 76	0.7773	0.7741	1.5
1.0134	1.0222	1.0183	1.75
1.1703	1.1349	1.1297	2

table used the previous mentioned references in another consideration. Although the first gander will tell us the more difference among the results of the present methodology with those obtained by [50, 51], the results can be proportionally acceptable.

To have a contradistinctive conceptualization about the OVFSDT in terms of electromagnetic nanoplates, [17] is employed. As long as the material is chosen electromagnetic in the current work, the mechanical behavior of this material is validated in table 3 for the present formulation. It is clearly visible that about the greater values of small scale factor as well as thinner plates, the results obtained by this paper are more adjacent to the ones obtained by [17]. As a rule, table 3 can confirm the accuracy of the results of the proposed formulation.

The benchmarked electromagnetic nanoplate employed in this paper has simply-supported boundary conditions and made of $BaTiO_3$-$CoFe_2O_4$ that the mechanical, electrical and magnetic properties are presented in table 4.

Various small scale cases versus variations of the magnetic and electric fields are considered by figures 2(a)–(c). In the first case (figure 2(a)), the higher-order nonlocality case is examined using several external electrical voltages. It is seen that with an increase in the higher-order nonlocal parameter the dynamic deflection's values are reducing but the influence is not as much as the increasing effect of the external voltage on the deflections. Second case (figure 2(b)) studies a specific condition within which the nonlocal case of Eringen is evaluated regarding $\mu_1 = l = 0$ nm. It is interesting to state that the outcomes of this figure are greater than those presented in the previous figure that will lead to a marked result that higher-order nonlocal strain gradient case makes nanoplate harder. This might be because of strain gradient length scale factor, but the higher-order nonlocality factor has a noticeable role in this category. The last case (figure 2(c)) shows the variations of the magnetic field. The figure presents that the nanoplate will be considerably impressed by a magnetic field rather than electric voltages. This can be observed due to the numerical gaps between the curves of figure 2(c) in comparison with the former figures. It can be concluded that the impacts of the electric field is less on the dynamic deflections than the magnetic field. It can be noted that increasing magnetic parameter decreased

Table 3. Comparisons of the non-dimensional biaxial critical biaxial buckling loads of fully simply-supported the electromagnetic plate computed by various plate theories ($h = 10$ nm, $\varphi_0 = -0.3$ V, $\psi_0 = 0.01$ A, $\Delta T = 100$ K, $\Gamma_0 = \mu_0/L_x$, $P_0 = N_0/A_{11}$) [52]. Reprinted from [52], Copyright (2018), with permission from Elsevier.

			Non-dimensional biaxial buckling load (P_0)				
			Non-dimensional nonlocal parameter (Γ_0)				
L_x/h	References	Theory	0	0.01	0.02	0.03	0.04
8	Present, ENET[*a] [17]-ENET[*a]	OVFSDT	21.4653	21.4586	21.3995	21.2211	20.9757
		KPT[*b]	23.9006	23.8593	23.7365	23.5349	23.2592
		MPT[*c]	21.8250	21.7877	21.6768	21.4948	21.2459
		RPT[*d]	21.8447	21.8074	21.6963	21.5141	21.2648
		PSDPT[*e]	21.8393	21.8020	21.6910	21.5088	21.2596
		TSDPT[*f]	21.8489	21.8116	21.7006	21.5183	21.2690
		HSDPT[*g]	21.8666	21.8294	21.7187	21.5370	21.2885
		ESDPT[*h]	21.8589	21.8216	21.7105	21.5282	21.2787
12	Present [17]	OVFSDT	26.7203	26.6820	26.5618	26.3590	26.1315
		KPT	27.6888	27.6475	27.5245	27.3228	27.0469
		MPT	26.6753	26.6360	26.5191	26.3273	26.0650
		RPT	26.6842	26.6449	26.5280	26.3361	26.0737
		PSDPT	26.6817	26.6425	26.5255	26.3337	26.0712
		TSDPT	26.6862	26.6469	26.5299	26.3380	26.0756
		HSDPT	26.6946	26.6553	26.5384	26.3466	26.0843
		ESDPT	26.6908	26.6515	26.5346	26.3426	26.0801
20	Present [17]	OVFSDT	39.7291	39.5684	39.4276	39.1298	38.8589
		KPT	39.8097	39.7683	39.6450	39.4427	39.1661
		MPT	39.3684	39.3280	39.2078	39.0106	38.7408
		RPT	39.3719	39.3315	39.2112	39.0140	38.7441
		PSDPT	39.3709	39.3305	39.2103	39.0130	38.7432
		TSDPT	39.3726	39.3322	39.2120	39.0147	38.7449
		HSDPT	39.3787	39.3389	39.2213	39.7208	38.7752
		ESDPT	39.3744	39.3340	39.2138	39.0165	38.7466
30	Present [17]	OVFSDT	44.8205	44.7622	44.6527	44.5038	44.2281
		KPT	45.9379	44.8576	44.7635	44.5699	44.4315
		MPT	44.9031	44.8627	44.7425	44.5453	44.2755
		RPT	44.9067	44.8663	44.7460	44.5488	44.2790
		PSDPT	44.9057	44.8653	44.7451	44.5478	44.2780
		TSDPT	44.9074	44.8670	44.7468	44.5496	44.2797
		HSDPT	44.9137	44.8741	44.7577	44.5599	44.2949
		ESDPT	44.9093	44.8689	44.7487	44.5514	44.2816

[a] Eringen's nonlocal elasticity theory ($\Gamma_0 \neq 0, \Gamma_1 = 0, l = 0$).

[b] Kirchhoff's plate theory.

[c] Mindlin's plate theory.

[d] Reddy's plate theory.

[e] Parabolic shear deformable plate theory.

[f] Trigonometric shear deformable plate theory.

[g] Hyperbolic shear deformable plate theory.

[h] Exponential shear deformable plate theory.

deflections that this is reversed about variations of the electric field. On the other hand, diminishing influence of nonlocality factors over these figures will lead to an interesting result that the impact of electric potential is more profound on the nonlocality than the magnetic one.

Figures 3(a) and (b) depict the lower-order nonlocal strain gradient condition versus variations of electric and magnetic fields. By looking at figures 2(c) and (b), it is seen that the magnetic field has more impacted on the strain gradient theory condition ($\mu_0 = \mu_1 = \mu, l = 0.5$ h) in comparison with Eringen's nonlocal elasticity theory condition ($\mu_1 = l = 0$ nm). In other words, the more changes in dynamic deflections of figure 3(b) than those in figure 2(c) lead to a significant conclusion that the decrease in deflections by nonlocal factor in the strain gradient case is more significant than the decrease in deflections by nonlocal factor in the Eringen's case. Figure 3(a) also demonstrates the changes in electric field for nonlocal strain gradient case in which the derived conclusions could be confirmed.

A general study on the excitation frequency of the electromagnetic nanoplate by change in some factors in the higher-order condition has been shown by figure 4. From all the figures, it can be vividly seen that when
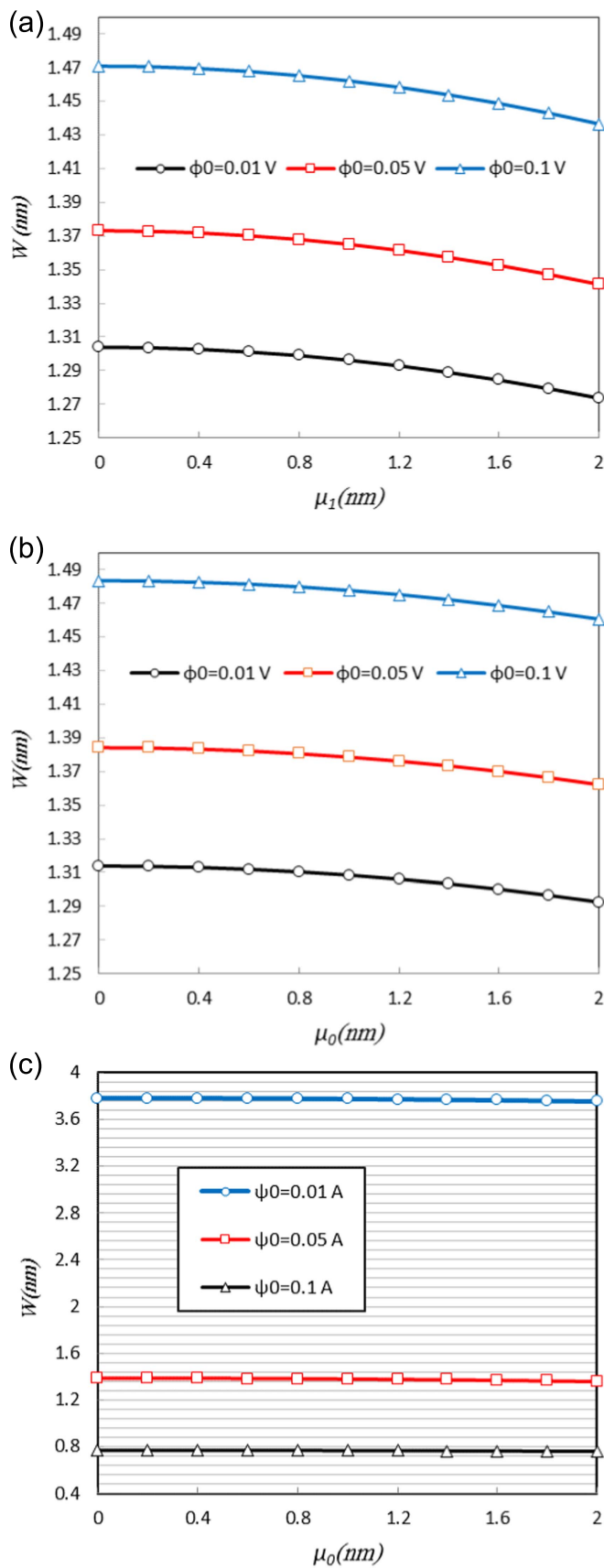
Figure 2. (a) Different values of the higher-order nonlocal parameter versus several external electric voltage ($\mu_0 = 0.2$ nm, $l = 0.5$ h, $\psi_0 = 0.05$ A, m $=$ n $= 1$, Δr $= 0.1$, $q_0 = 0.05$ GPa, $x_0 = y_0 = 0.5L_x$, $c_1 = c_2 = L_x$). (b) Different values of the nonlocal parameter versus several external electric voltage ($\mu_1 = l = 0$ nm, $\psi_0 = 0.05$ A, m $=$ n $= 1$, Δr $= 0.1$, $q_0 = 0.05$ GPa, $x_0 = y_0 = 0.5L_x$, $c_1 = c_2 = L_x$). (c) Different values of the lower-order nonlocal parameter versus several external magnetic potential ($\mu_1 = l = 0$ nm, $\varphi_0 = 0.05$ V, m $=$ n $= 1$, Δr $= 0.1$, $q_0 = 0.05$ GPa, $x_0 = y_0 = 0.5L_x$, $c_1 = c_2 = L_x$).
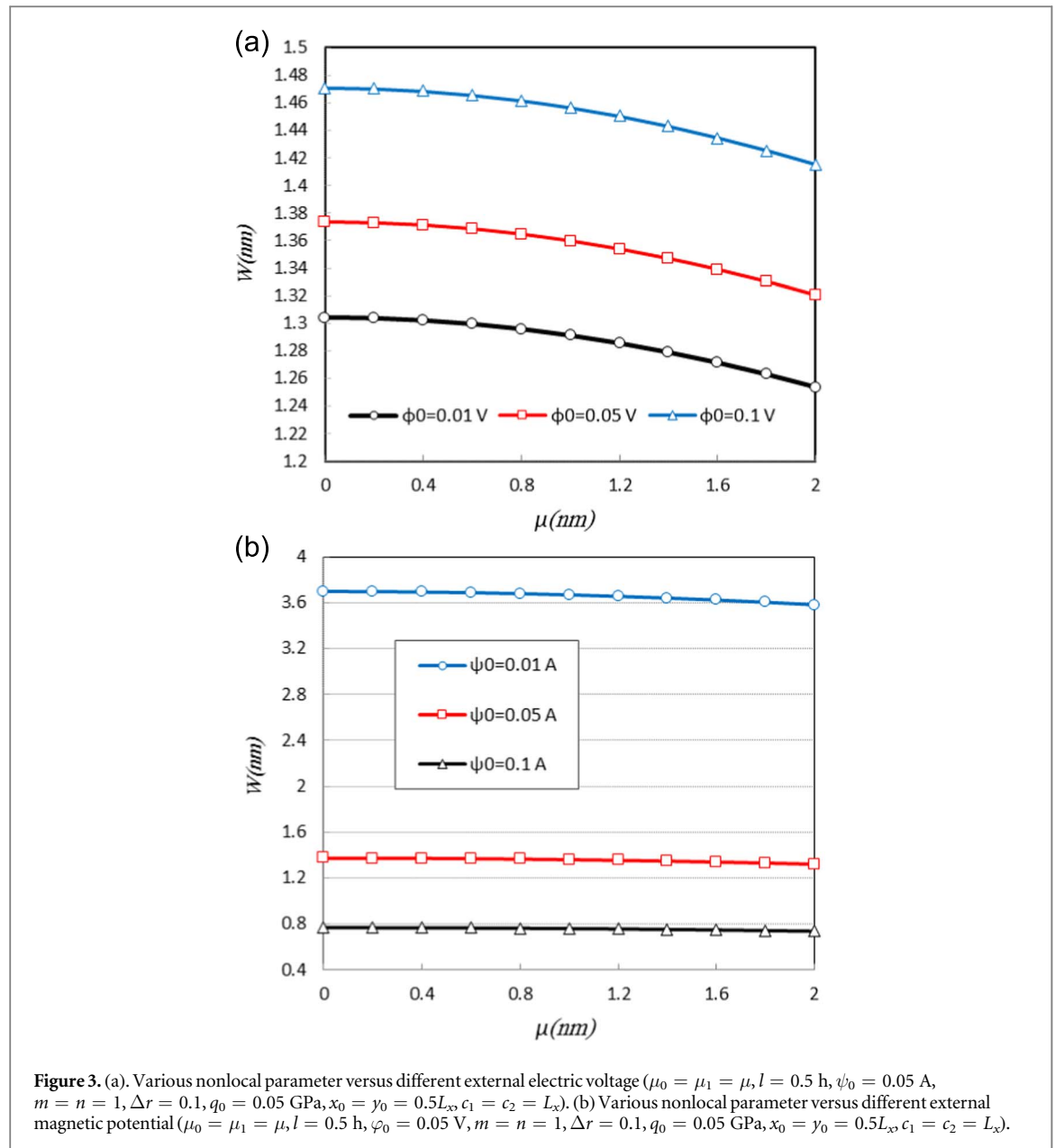
Figure 3. (a). Various nonlocal parameter versus different external electric voltage ($\mu_0 = \mu_1 = \mu, l = 0.5$ h, $\psi_0 = 0.05$ A, $m = n = 1, \Delta r = 0.1, q_0 = 0.05$ GPa, $x_0 = y_0 = 0.5 L_x, c_1 = c_2 = L_x$). (b) Various nonlocal parameter versus different external magnetic potential ($\mu_0 = \mu_1 = \mu, l = 0.5$ h, $\varphi_0 = 0.05$ V, $m = n = 1, \Delta r = 0.1, q_0 = 0.05$ GPa, $x_0 = y_0 = 0.5 L_x, c_1 = c_2 = L_x$).

Table 4. Properties of BaTiO$_3$-CoFe$_2$O$_4$ nanoplate [52–56].

Elastic properties (GPa)

$C_{11} = C_{22} = 226, C_{12} = 125, C_{13} = C_{23} = 124, C_{33} = 216, C_{44} = C_{55} = 44.2, C_{66} = 50.5$
Piezoelectric quantities (C m^{-2})
$e_{31} = e_{32} = -2.2, e_{15} = e_{24} = 5.8, e_{33} = 9.3$
Dielectric quantities ($C/V.m$)
$\kappa_{11} = \kappa_{22} = 5.64e$-9, $\kappa_{33} = 6.35e$-9
Piezomagnetic quantities ($N/A.m$)
$q_{31} = q_{32} = 290.1, q_{33} = 349.9, q_{15} = 275$
Magnetoelectric quantities ($N.s/V.C$)
$d_{11} = d_{22} = 5.367e$-12, $d_{33} = 2737.5e$-12
Magnetic quantities ($N.s^2/C^2$)
$\eta_{11} = \eta_{22} = -297e$-6, $\eta_{33} = 83.5e$-6
Other quantities
$h = 4$ nm, $Lx = Ly = 60$ nm, $\rho = 5.55e + 3$(kg m^{-3})

$\Delta r = 1$ the plate passes through resonance conditions. It can also be seen that the dynamic deflections after resonance area are less than previous values and they become smaller and smaller when frequency ratio is further away from 1. Obviously, by assessing infinite values of excitation frequencies, the deflection values are very small
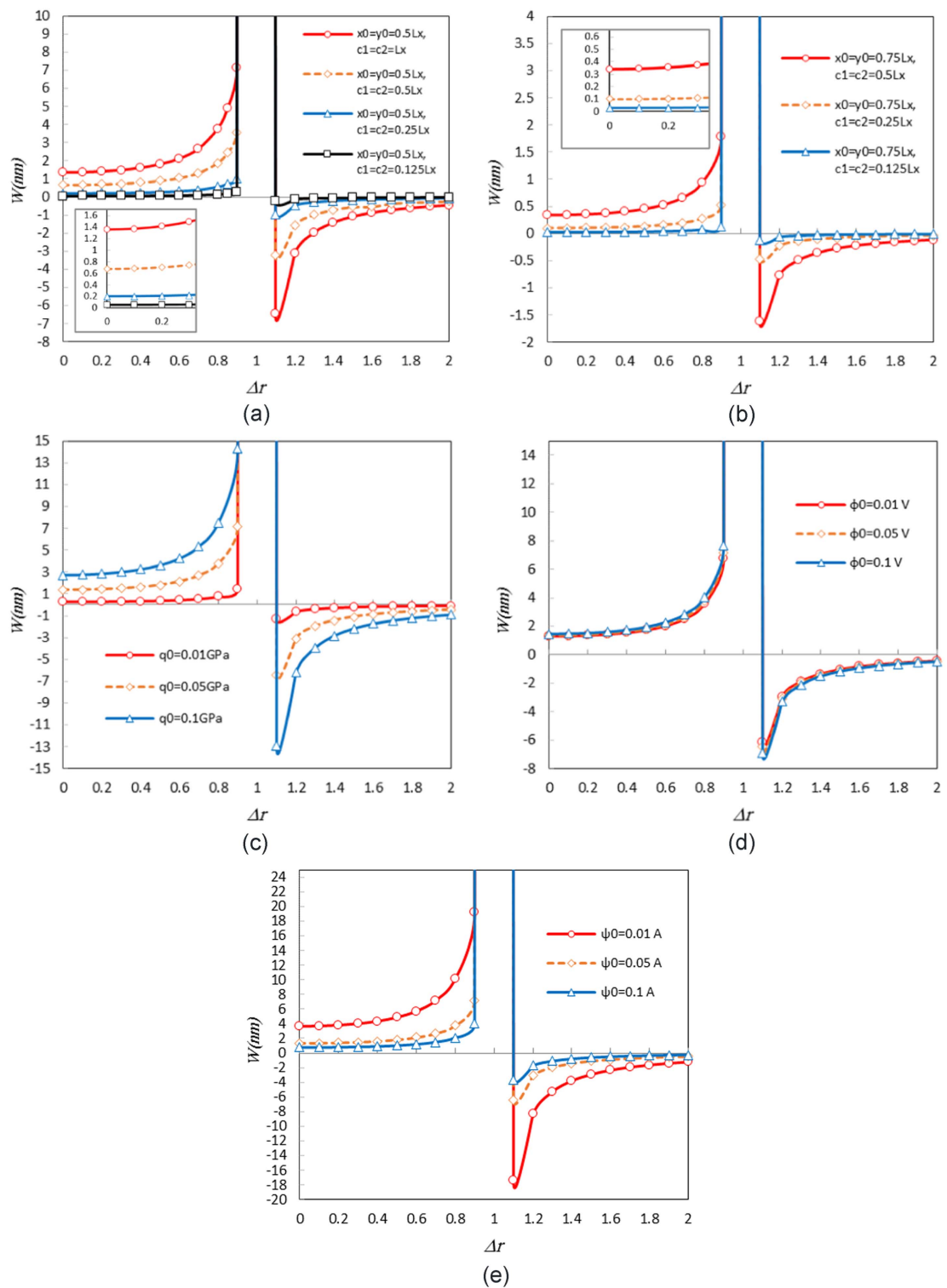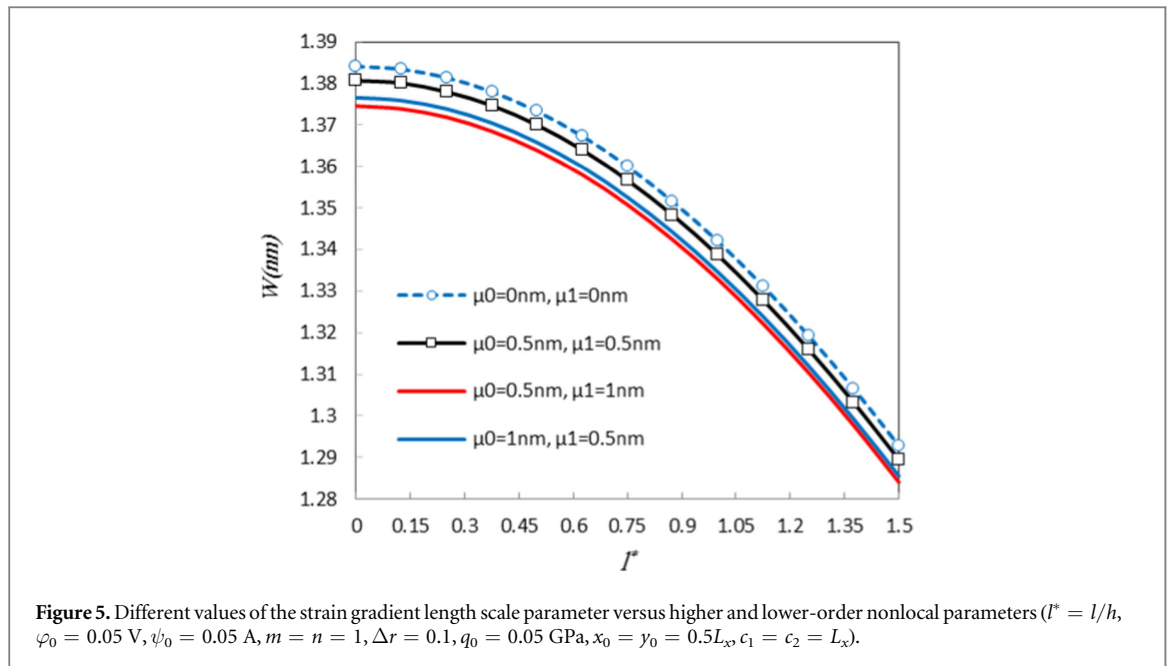
Figure 4. (a) Several frequency ratio versus various distributed loads ($\mu_0 = 0.2$ nm, $\mu_1 = 0.4$ nm, $l = 0.5$ h, $\varphi_0 = 0.05$ V, $\psi_0 = 0.05$ A, $q_0 = 0.05$ GPa). (b) Several frequency ratio versus various distributed loads ($\mu_0 = 0.2$ nm, $\mu_1 = 0.4$ nm, $l = 0.5$ h, $\varphi_0 = 0.05$ V, $\psi_0 = 0.05$ A, $q_0 = 0.05$ GPa). (c) Several frequency ratio versus various load value ($\mu_0 = 0.2$ nm, $\mu_1 = 0.4$ nm, $l = 0.5$ h, $\varphi_0 = 0.05$ V, $\psi_0 = 0.05$ A, $x_0 = y_0 = 0.5L_x, c_1 = c_2 = L_x$). (d) Several frequency ratio versus various electric voltages ($\mu_0 = 0.2$ nm, $\mu_1 = 0.4$ nm, $l = 0.5$ h, $\psi_0 = 0.05$ A, $q_0 = 0.05$ GPa, $x_0 = y_0 = 0.5L_x, c_1 = c_2 = L_x$). (e) Several frequency ratio versus various magnetic potentials ($\mu_0 = 0.2$ nm, $\mu_1 = 0.4$ nm, $l = 0.5$ h, $\varphi_0 = 0.05$ V, $q_0 = 0.05$ GPa, $x_0 = y_0 = 0.5L_x$, $c_1 = c_2 = L_x$).

which means that the plate does not have a vibrational behavior. From figure 4(a), it is shown that whatever the distribution area of the harmonic load is smaller the deflections are smaller. Moreover, by comparing figures 4(a) and (b), it is vivid that whatever the centroid of the load distribution is getting farther from the center of the plate, the dynamic deflection values have become smaller. The influence of the transverse load is

Figure 5. Different values of the strain gradient length scale parameter versus higher and lower-order nonlocal parameters ($l^* = l/h$, $\varphi_0 = 0.05$ V, $\psi_0 = 0.05$ A, $m = n = 1$, $\Delta r = 0.1$, $q_0 = 0.05$ GPa, $x_0 = y_0 = 0.5L_x$, $c_1 = c_2 = L_x$).

considered by figure 4(c). It is shown that increase of the transverse load increases dynamic deflections and this will be more intensified after $\Delta r = 0.4$ for bigger loads. It can be stated that with increase in the transverse load, the effect of excitation frequency will be greater on the deflections. Additionally, figures 4(d) and (e) studied the effects of magnetic and electric fields by the variations of the frequency ratio. It is simply seen that the magnetic field has further impact on the vibrational behavior of the nanoplate than the electric one. It was concluded from the last figure and here this conclusion is more confirmed.

A study in terms of higher-order nonlocal conditions is presented in figure 5. As a matter of fact the parameters μ_0, μ_1, *and l* are compared in a special case. It is worth noting that when the case of $\mu_0 = 0.5$ nm, $\mu_1 = 1$ nm and $\mu_0 = 1$ nm, $\mu_1 = 0.5$ nm are taken into consideration, increasing the value of the strain gradient length scale factor makes the results of two nearby cases closer to one another. It can be concluded that whenever the nanoplate's stiffness is greater, the use of higher-order nonlocal strain gradient conditions cannot be important. It can be also seen that in condition of $\mu_0 = 0$ nm, $\mu_1 = 0$ nm where the stress nonlocality is ignored, the deflections are largest values.

5. Conclusions

This research has discussed forced vibrations of a piezoelectric-piezomagnetic nanoplate under external electric and magnetic fields whilst a new first-order shear deformation theory was proposed. The higher-order nonlocal strain gradient theory was evaluated to consider the effects of quantum in a small scale. Moreover, an analytical solution was employed to present the numerical results. By comparing the results obtained from the present theory for various benchmarked nanoplates with those obtained from several well-known theories in literature, the accuracy of the present theory was justified. Finally, with regard to the notable results, the following phrases are addressed as significant outcomes in the current article:

- The effects of magnetic field are remarkably further on the vibrational behavior of the nanoplate than the electric field influences.

- Increasing magnetic field decreases dynamic deflections and vice versa with an increase in the electric potential the deflections will be increased.

- The impact of electric potential on the nonlocality is more profound than the magnetic one.

- Strain gradient length scale parameter increases the stiffness of the nanoplate and decreases the maximum dynamic deflections.

- It is interesting to declare that by increasing stiffness of the nanoplate the results of higher and lower-order nonlocal parameters will be similar to each other.

Acknowledgments

ORCID iDs

Mohammad Malikan https://orcid.org/0000-0001-7356-2168
Francesco Tornabene https://orcid.org/0000-0002-5968-3382

References

[1] Estevez J M G 2014 *Nanomagnetism* (Altrincham, Cheshire, UK: One Central Press (OCP))
[2] Himpsel F J *et al* 1998 Magnetic nanostructures *Adv. in phys.* **47** 511–97
[3] Cardona M 1965 Optical properties and band structure of $SrTiO_3$ and $BaTiO_3$ *Phys. Rev.* **A140** 651
[4] Bauerle D, Braun W, Sprussel G and Koch E E 1978 Vacuum ultraviolet reflectivity and band structure of $SrTiO_3$ and $BaTiO_3$ *Phys. B* **29** 179–84
[5] Mitsui T and Westphal W B 1961 Dielectric and x-ray studies of $Ca_xBa_{1-x}TiO_3$ and $Ca_xSr_{1-x}TiO_3$ *Phys. Rev.* **124** 1354
[6] Avellaneda M and Harshe G 1994 Magnetoelectric effect in piezoelectric/magnetostrictive multilayer (2-2) *composites, J of Intelligent Mater. Syst. and Struct.* **5** 501–13
[7] Srinivasan G, Rasmussen E T, Gallegos J and Srinivasan R 2001 Magnetoelectric bilayer and multilayer structures of magnetostrictive and piezoelectric oxides *Phys. Review* B **64** 1–6
[8] Lopatina S, Lopatina I and Lisnevskaya S I 1994 Magnetoelectric PZT/ferrite composite material *Ferroelectrics* **162** 63–8
[9] Nan C-W 1994 Magnetoelectric effect in composites of piezoelectric and piezomagnetic phases *Phys. Review* B **50** 6082–8
[10] De Jonghie L C and Rahman M N 2003 Sintering of Ceramics *Handbook of Advanced Ceramics* vol I (Cambridge, MA: Academic Press) ch 4 pp 187–264
[11] Ke L L, Wang Y S and Wang Z D 2012 Nonlinear vibration of the piezoelectric nanobeams based on the nonlocal theory *Compos. Struct.* **94** 2038–47
[12] Liu C, Ke L L, Wang Y S, Yang J and Kitipornchai S 2014 Buckling and post-buckling of size-dependent piezoelectric Timoshenko nanobeams subject to thermo-electro-mechanical loadings *Int. J. Struct. Stab. Dy.* **14** 1350067
[13] Jiang L Y and Yan Z 2012 Vibration and buckling analysis of a piezoelectric nanoplate considering surface effects and in-plane constraints *Proc. R. Soc.* A **468** 3458–75
[14] Fang X-Q and Zhu C-S 2017 Size-dependent nonlinear vibration of nonhomogeneous shell embedded with a piezoelectric layer based on surface/interface theory *Compos. Struct.* **160** 1191–7
[15] Zhu C-S, Fang X-Q, Liu J-X and Li H-Y 2017 Surface energy effect on nonlinear free vibration behavior of orthotropic piezoelectric cylindrical nano-shells *Euro. J. of Mech. A/Solids* **66** 423–32
[16] Jamalpoor A, Ahmadi-Savadkoohi A, Hossein M and Hosseini-Hashemi S 2017 Free vibration and biaxial buckling analysis of double magneto-electro-elastic nanoplate-systems coupled by a Visco-Pasternak medium via nonlocal elasticity theory *Euro. J of Mech./A Solids* **63** 84–98
[17] Gholami R and Ansari R 2017 A unified nonlocal nonlinear higher-order shear deformable plate model for postbuckling analysis of piezoelectric-piezomagnetic rectangular nanoplates with various edge supports *Compos. Struct.* **166** 202–18
[18] Arefi M and Zenkour A M 2017 Size-dependent free vibration and dynamic analyses of piezo-electro-magnetic sandwich nanoplates resting on viscoelastic foundation *Physica B: Physics of Condensed Matter* **521** 188–97
[19] Barati M R and Shahverdi H 2018 A general nonlocal stress-strain gradient theory for forced vibration analysis of heterogeneous nanoporous plates *Euro. J of Mech./A Solids* **67** 215–30
[20] Ebrahimi F and Barati M R 2018 Damping vibration analysis of graphene sheets on viscoelastic medium incorporating hygro-thermal effects employing nonlocal strain gradient theory *Compos. Struct.* **185** 241–53
[21] Kamarian S, Salim M, Dimitri R and Tornabene F 2016 Free vibration analysis of conical shells reinforced with agglomerated carbon nanotubes *Int. J. Mech. Sci.* **108–109** 157–65
[22] Tornabene F, Fantuzzi N and Bacciocchi M 2014 Free vibrations of free-form doubly-curved shells made of functionally graded materials using higher-order equivalent single layer theories *Compos. Part B-Eng.* **67** 490–509
[23] Tornabene F, Fantuzzi N, Bacciocchi M and Viola E 2016 Effect of agglomeration on the natural frequencies of functionally graded carbon nanotube-reinforced laminated composite doubly-curved shells *Compos. Part B-Eng.* **89** 187–218
[24] Banić D, Bacciocchi M, Tornabene F and Ferreira A J M 2017 Influence of winkler-pasternak foundation on the vibrational behavior of plates and shells reinforced by agglomerated carbon nanotubes *Appl. Sci.* **7** 1228
[25] Fantuzzi N, Tornabene F, Bacciocchi M and Dimitri R 2017 Free vibration analysis of arbitrarily shaped functionally graded carbon nanotube-reinforced plates *Compos. Part B-Eng.* **115** 384–408
[26] Nejati M, Asanjarani A, Dimitri R and Tornabene F 2017 Static and free vibration analysis of functionally graded conical shells reinforced by carbon nanotubes *Int. J. Mech. Sci.* **130** 383–98
[27] Nejati M, Dimitri R, Tornabene F and Hossein Y M 2017 Thermal buckling of nanocomposite stiffened cylindrical shells reinforced by functionally graded wavy carbon nano-tubes with temperature-dependent properties *Appl. Sci.* **7** 1223
[28] Tornabene F, Fantuzzi N and Bacciocchi M 2017 Linear static response of nanocomposite plates and shells reinforced by agglomerated carbon nanotubes *Compos. Part B-Eng.* **115** 449–76
[29] Tornabene F, Bacciocchi M, Fantuzzi N and Reddy J N 2017 Multiscale approach for three-phase CNT/polymer/fiber laminated nanocomposite structures *Polym. Composite* Accepted (https://doi.org/10.1002/pc.24520)
[30] She G L, Shu X and Ren Y R 2016 Thermal buckling and postbuckling analysis of piezoelectric FGM beams based on high-order shear deformation theory *J. Therm. Stresses* **40** 783–97
[31] She G L, Yuan F G and Ren Y R 2017 Nonlinear analysis of bending, thermal buckling and post-buckling for functionally graded tubes by using a refined beam theory *Compos. Struct.* **165** 74–82

[32] She G L, Yuan F G and Ren Y R 2017 Research on nonlinear bending behaviors of FGM infinite cylindrical shallow shells resting on elastic foundations in thermal environments *Compos. Struct.* **170** 111–21

[33] She G L, Yuan F G and Ren Y R 2017 Thermal buckling and post-buckling analysis of functionally graded beams based on a general higher-order shear deformation theory *Appl. Math. Modell.* **47** 340–57

[34] She G L, Yuan F G, Ren Y R and Xiao W S 2017 On buckling and postbuckling behavior of nanotubes *Int. J. of Eng. Sci.* **121** 130–42

[35] She G L, Ren Y R, Yuan F G and Xiao W S 2018 On vibrations of porous nanotubes *Int. J. of Eng. Sci.* **125** 23–35

[36] Malikan M, Jabbarzadeh M and Dastjerdi S 2017 Non-linear Static stability of bi-layer carbon nanosheets resting on an elastic matrix under various types of in-plane shearing loads in thermo-elasticity using nonlocal continuum *Microsyst. Tech.* **23** 2973–91

[37] Malikan M 2017 Electro-mechanical shear buckling of piezoelectric nanoplate using modified couple stress theory based on simplified first order shear deformation theory *Appl. Math. Modell.* **48** 196–207

[38] Malikan M 2017 Analytical predictions for the buckling of a nanoplate subjected to nonuniform compression based on the four-variable plate theory *J. of Appl. and Comput. Mech.* **3** 218–28

[39] Malikan M 2018 Buckling analysis of a micro composite plate with nano coating based on the modified couple stress theory *J. of Appl. and Comput. Mech.* **4** 1–15

[40] Shimpi R P 2002 Refined plate theory and its variants *AIAA Journal* **40** 137–46

[41] Malikan M 2018 Temperature influences on shear stability of a nanosize plate with piezoelectricity effect *Multidiscip. Model. Mater. Struct.* **14** 125–42

[42] Golmakani M E, Malikan M, Sadraee Far M N and Majidi H R 2018 Bending and buckling formulation of graphene sheets based on nonlocal simple first order shear deformation theory *Mater. Res. Express* **5** 065010

[43] Malikan M and Sadraee Far M N 2018 Differential quadrature method for dynamic buckling of graphene sheet coupled by a viscoelastic medium using neperian frequency based on nonlocal elasticity theory *J. of Appl. and Comput. Mech.* **4** 147–60

[44] Liu C, Ke L L, Yang J, Kitipornchai S and Wang Y S 2016 Buckling and post-buckling analysis of size-dependent piezoelectric nanoplates *Theo. & Appl. Mech. Lett.* **6** 253–67

[45] Zhang D P, Lei Y J and Shen Z B 2017 Thermo-electro-mechanical vibration analysis of piezoelectric nanoplates resting on viscoelastic foundation with various boundary conditions *Inter. J of Mech. Sci.* **131–132** 1001–15

[46] Lim C W, Zhang G and Reddy J N 2015 A Higher-order nonlocal elasticity and strain gradient theory and its applications in wave propagation *J of the Mech. and Phys. of Solids* **78** 298–313

[47] Nematollahi M S, Mohammadi H and Nematollahi M A 2017 Thermal vibration analysis of nanoplates based on the higher-order nonlocal strain gradient theory by an analytical approach *Superlattices and Microstruct.* **111** 944–59

[48] Farajpour A, Haeri Yazdi M R, Rastgoo A and Mohammadi M 2016 A higher-order nonlocal strain gradient plate model for buckling of orthotropic nanoplates in thermal environment *Acta Mech.* **227** 1849–67

[49] Golmakani M E and Rezatalab J 2015 Nonuniform biaxial buckling of orthotropic Nano plates embedded in an elastic medium based on nonlocal Mindlin plate theory *Compos. Struct.* **119** 238–50

[50] Golmakani M E and Far M N S 2017 Buckling analysis of biaxially compressed double-layered graphene sheets with various boundary conditions based on nonlocal elasticity theory *Microsyst. Technol.* **23** 2145–61

[51] Ansari R and Sahmani S 2013 Prediction of biaxial buckling behavior of single-layered graphene sheets based on nonlocal plate models and molecular dynamics simulations *Appl. Math. Modell.* **37** 7338–51

[52] Malikan M and Nguyen V B 2018 Buckling analysis of piezo-magnetoelectric nanoplates in hygrothermal environment based on a novel one variable plate theory combining with higher-order nonlocal strain gradient theory *Phys. E: Low-dimens. Syst. and Nanostruct.* **102** 8–28

[53] Ke L L, Wang Y S, Yang J and Kitipornchai S 2014 Free vibration of size-dependent magneto-electro-elastic nanoplates based on the nonlocal theory *Acta Mech. Sin.* **30** 516–25

[54] Farajpour A, Rastgoo A and Farajpour M R 2017 Nonlinear buckling analysis of magneto-electro-elastic CNT-MT hybrid nanoshells based on the nonlocal continuum mechanics *Compos. Struct.* **180** 179–91

[55] Zenkour A M and Sobhy M 2018 Nonlocal piezo-hygrothermal analysis for vibration characteristics of a piezoelectric Kelvin–Voigt viscoelastic nanoplate embedded in a viscoelastic medium *Acta Mech.* **229** 3–19

[56] Farajpour M, Hairi Yazdi M R, Rastgoo A, Loghmani M and Mohammadi M 2016 Nonlocal nonlinear plate model for large amplitude vibration of magneto-electro-elastic nanoplates *Compos. Struct.* **140** 323–36